The timing and ecological consequences of Pleistocene megafaunal decline in the eastern Andes of Colombia

Declaration of work

Submitted by Felix Conor Pym

to the University of Exeter as a thesis for the degree of

Masters of Science by Research in Geography

August 2022

I certify that all material in this thesis which is not my own work has been identified and that any material that has previously been submitted and approved for the award of a degree by this or any other University has been acknowledged.

ABSTRACT

Examining the ecological consequences of Late-Quaternary megafaunal extinctions within biodiversity hotspots is crucial for our understanding of the potential consequences of contemporary extinctions. This research presents the first multi-species record of spores of coprophilous fungi (SCF) from Monquentiva and the high Andean forests of Colombia to reconstruct the Late-Pleistocene and Holocene megafaunal abundance. Fossilised pollen and charcoal are used to examine the consequences of megafaunal declines on the history of the study region. The SCF record indicated the presence of megafauna since at least 30,290 BP; with two periods of megafauna decline at ca. 22,900 and 10,990 BP. At Monquentiva, megafaunal decline in the Early-Holocene resulted in transitional non-analogue vegetation, a loss of some herbivore-dispersed taxa, an encroachment of some palatable and woody flora, and a rise in fire activity. Overall, this research shows that ecosystems in the eastern Colombian Cordillera were highly sensitive to the decline of megafaunal populations. Under the current biodiversity crisis, management and conservation efforts must account for the effect of local herbivore declines on the dispersal of certain plant species, on fire activity and the potential loss of ecosystem services.

Keywords: Pleistocene-Holocene transition; Palaeoecology; Colombian Andes; Coprophilous fungi spores; Megafaunal decline; *Sporormiella*; Multiproxy; Vegetation; Fire.

TABLE OF CONTENTS

LIST OF FIGURES

LIST OF TABLES

APPENDICES

ACKNOWLEDGEMENTS

The research conducted in this thesis was possible thanks to the BioResilience project (https://blogs.exeter.ac.uk/bioresilience/) (see funding section). The BioResilience project looked to examine the long-term resilience of Colombian forest ecosystems to environmental and climatic changes and improve the understanding of the future implications of forest degradation for Colombian society. It is through the palaeoecological component of the project that we were able to investigate long-term ecological changes using lake sedimentary records.

The completion of this thesis would not be possible without the individuals who have supported and guided me throughout. Here I attempt to show a degree of the appreciation I have for you all.

I begin by expressing my highest level of gratitude to my supervisor Dr Dunia H. Urrego, the catalyst of my research journey. You have installed more trust in me than I could ever have asked, continually shared your knowledge and given me a wealth of extraordinary opportunities. It is difficult to put into words how grateful I am that our paths crossed. Thank you! It is my ambition that one day I can repay what you have done for me. With this in mind, I would like to share a photo to the reader of Dunia guiding me through the lake-coring process using a Livingston piston corer (Colinvaux *et al.,* 1999; photo captured by AmazInk, 2022).

I also owe a lot of gratitude to my co-supervisor Dr Felipe Franco-Gaviria (also pictured). I thank you for the time, energy and patience you spent on me in the laboratories, on zoom calls and in the field. I thank you for your companionship during the pandemic (even if it meant an early lunch), for always being available and most of all for becoming un amigo.

To the people that assisted during the development of the research, I pay my thanks to the support of Angela Elliot, Joana Zaragoza-Castells and the whole laboratory technician team in the Physical Geography department at the University of Exeter. I would also like to thank Yvonne Marcela Castaneda Riascos for helping with the identification of pollen taxa, Alex Room for his help with regime shift analysis, Anggi Hapsari in assisting with Oxcal uncertainty dating and Nathaniel Reid for support with RStudio.

To the long-term members of the PalaeoTea research group: Jack Oughton, Ismael Garcia Espinoza and Anggi Hapsari. Thank you for your friendship, the countless activities and sense of community. I pay special thanks to Ismael for your contribution to the publication, for sharing your passion and knowledge of figure design and for becoming a good friend in the field.

I would also like to thank Dr Barend van Maanen and the MANGROOVIE project for allowing me to assist in targeted fieldwork upon the mangrove ecosystems of Colombia. I hope that my efforts showed some of the gratification I have. Without this opportunity and the trust of Dunia Urrego and Barend van Maanen, I would not have been able to experience the ecosystem of Monquentiva (the study site of this thesis) and the breath-taking beauty of Colombia.

Upon this fieldwork, I had the pleasure of meeting a number of wonderful people to whom I owe thanks. To Mónica Amador-Jiménez, Mauricio Naranjo and Luisa Fernanda Gomez Vargas. Thank you for welcoming me to Colombia, for sharing your time with me and for your enthusiasm and commitments in the field. A special thank you to Luisa, for being my guide, for your values and kind-heartedness and for your support and motivation when writing the publication. To the anglers of Barranquilla and the conservationists and farmers of Tenasucã and Monquentiva. Thank you for your acceptance, your patience with my Spanish and teamwork in the field. I hope to meet you all again in the future.

AUTHORS' DECLARATION

This thesis manuscript is comprised of a supplemented publication (Pym *et al.,* 2022). The following declaration summarises a statement from the thesis author regarding the contributions made to the thesis and to the co-authored publication. We certify that the manuscript author led the completion of the supplemented thesis. The contributions made in the development of the publication are as followed:

Felix Pym: Conceptualization, Methodology, Software, Validation, Formal analysis, Investigation, Writing – Original Draft, Writing – Review & Editing. **Felipe Franco-Gaviria:** Methodology, Software, Formal analysis, Writing – Review & Editing. **Ismael G. Espinoza:** Investigation, Visualisation, Writing – Review & Editing. **Dunia H. Urrego:** Supervision, Funding acquisition, Conceptualization, Methodology, Validation, Writing – Review & Editing. All authors supported the production process and approved the ideas for its publication.

DEFINITIONS, ABBREVIATIONS AND SYMBOLS

Term	Definition
SCF	Spores of coprophilous fungi
Key SCF	All identifiable spores of coprophilous and semi-coprophilous fungi grouped to create a sum of spores associated with megafaunal abundance

Abbreviation	Meaning
Cal yr BP	Radiocarbon dated (^{14}C) years before present
TPA	Total pollen assemblage
ITCZ	Intertropical Convergence Zone
ENSO	El Niño-Southern Oscillation
STARS	Sequential t-test analysis of regime shifts
RSI	Regime shift index
CCA	Canonical correspondence analysis
CHAR	Interpolated charcoal concentration
BP	Calendar years before present

Symbol	Meaning
ha	hectares
km	Kilometre
masl	Metres above sea level (m)
cm	Centimetre
µm	Micrometres

1. INTRODUCTION

Megafauna include mammals that weigh over 45 kg and as ecological keystone species, they can have an important ecological role in shaping habitats and entire ecosystems (Martin and Klein, 1984; Mills *et al.*, 1993; Gill *et al.,* 2009). Megafauna can modify vegetation composition (Gordon *et al.,* 2021), influence seed-dispersal (Peres *et al.,* 2016), maintain flora coexistence (Sankaran *et al.,* 2005), shape soil nutrients and fertility (Wigley *et al.,* 2020) and suppress fire activity (Waldram *et al.,* 2008). In modern savannas, antelope-induced grazing suppresses grass and tree growth (Staver and Bond, 2014) while rhinos can limit fire activity by feeding on grasses and controlling fuel build-up (Waldram *et al.,* 2008). A large proportion of megafaunal species went extinct on all continents during the Pleistocene (Barnosky *et al.,* 2004), and given their ecological importance the consequences of these extinctions are thought to be significant (Johnson, 2009; Malhi *et al.,* 2016). The cause of extinction remains debated; however, studies have linked climatic changes, human activity and even an extra-terrestrial impact to their decline (Firestone *et al.,* 2007; Cooper *et al.,* 2015; Raczka *et al.,* 2019). South America lost an estimated 80% of its megafauna, including ground sloths (*Megatherium americanum*) and glyptodons (*Glyptodon clavipes*) (Barnosky *et al.,* 2004; Wroe *et al.,* 2004; Lima-Ribeiro and Diniz-Filho, 2013) (Fig. 1). Despite experiencing one of the most significant declines of megafaunal species, information about South American megafaunal extinctions remains limited.

Figure 1. An artist illustration of some South American Pleistocene megafaunal species that inhabited Colombia (Carreño, 2017).

The record of extinction in South America

The timing of the Pleistocene megafaunal extinction in South America is yet to be determined as records are scarce (e.g. Elias and Schreve, 2007; Rozas-Dávila *et al.,* 2016; Raczka *et al.,* 2018; Raczka *et al.,* 2019). In North America, robust archaeological evidence suggests the timing of megafaunal extinction between 11,500 and 11,000 years ago (Barnosky *et al.,* 2004). However, extinctions may have occurred earlier, between 14,000 - 12,700 cal yr BP (calibrated years before present, hereafter BP) (Robinson *et al*., 2005; Gill *et al.,* 2009; 2012; Perrotti*,* 2018). Perhaps in relation to overhunting resulting from humans arriving in North America as early as 15,500 years ago (Waters *et al.,* 2011). In South America, the extinction window has been suggested to have occurred between 15,000 and 10,000 years ago (Barnosky *et al.,* 2004). The limited records available suggest variability in megafaunal extinction timings. In the Peruvian Andes, researchers found the local extinction occurring as early as 15,800 BP (Rozas-Dávila *et al.,* 2016). Whereas in the Ecuadorian Andes extinction was recorded much later, by 12,800 BP (Raczka *et al.,* 2019). This timing is similar to the extinction recorded in the Brazilian cerrado lowlands, reached by 12,000 BP (Raczka *et al.,* 2018). However, in Argentina and Brazil fossilised megafaunal bones have been dated to the early-Holocene as late as 6560 BP (Borrero *et al.,* 1998; Steadman *et al.,* 2007). Thus, suggesting the early-Holocene survival of some megafauna (Neves and Piló, 2003). The available information in South America leaves a broad range, between 15,800 - 6560 BP, on the timing of Pleistocene megafaunal decline in the region and within different ecosystems.

The ecological consequences of extinction

Late-Pleistocene megafaunal extinctions likely had significant ecological consequences on the ecosystems we know today but available records vary. The extinction of the megafauna in North America led to the formation of flora without modern analogues (hereafter non-analogue) and increased fire activity (Gill *et al.,* 2009, 2012). In the Peruvian Andes, the collapse of megafauna was followed by a rise in fire activity and species turnover (Rozas-Dávila *et al.,* 2016). In the Pampas lowlands, megafaunal loss was apparently not associated with the expected rise in shrubby vegetation and fire activity was not observed in the record (Prieto, 2000). In the Brazilian cerrado, the ecosystem remained largely stable but experienced an increase in some palatable species (Raczka *et al.,* 2018). Despite these recent advancements, it remains unclear what the ecological consequences of extinctions were in other high biodiversity regions of South America or whether these consequences were habitat specific.

Spores of coprophilous fungi (SCF)

Research of the Pleistocene megafaunal extinction and their impact on the Quaternary landscape in South America has used radiocarbon-dated bone remains recovered from, for example, archaeological sites (Borrero, 2009; Barnosky and Lindsey, 2010; Lima-Ribeiro and Diniz-Filho, 2013). The collagen extracted from fossilised bones provides accurate dating, however, they are rare, isolated and often, geographically concentrated (Johnson *et al.,* 2015; van Asperen *et al.,* 2020). The use of spores of coprophilous fungi (SCF) to reconstruct megafaunal presence can reduce these limitations because they preserve well in stratigraphic units where chronological frameworks can be built using several ages (van Geel *et al.,* 2007; 2011; Lee *et al.,* 2022). SCF grow and reproduce on herbivore faeces, they are spread to surrounding vegetation where they can be ingested and excreted by megafauna (Davis and Shafer, 2006; Perrotti and van Asperen, 2019) (Fig. 2). Therefore making SCF a reliable indicator for the presence/absence and abundance of megafauna (Wood and Wilmshurst, 2013; Johnson *et al*., 2015). SCF such as *Sporormiella* can also reproduce in the dung of smaller herbivores (Feranec *et al.,* 2011). However, SCF reproduction is limited to the size of the faeces (Halbwachs and Bässler, 2020). Therefore, due to the comparative volume of dung produced, the contribution made to the production of SCF by megafauna overrules any signal associated with these smaller fauna (Gill *et al.,* 2013; Lee *et al.,* 2022). SCF can be found in conjunction with other palaeoecological proxies including pollen and charcoal allowing an understanding of the consequences of megafaunal extinctions on vegetation and fire activity (Raczka *et al.,* 2018; van Asperen *et al.,* 2020).

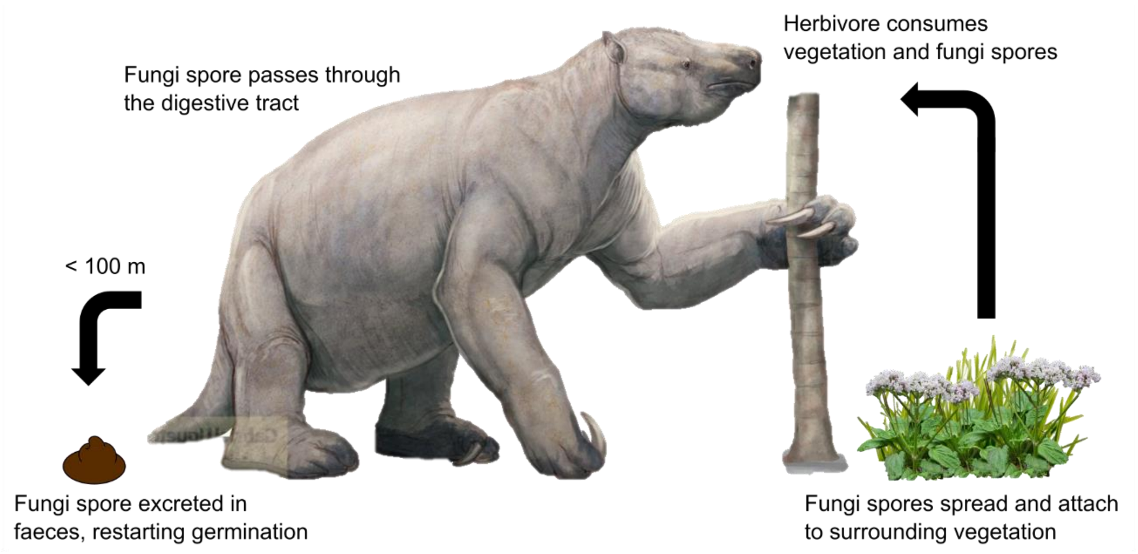

Figure 2. Generalised recreation of the lifecycle of spores of coprophilous fungi (SCF). The depiction is based on descriptive spore lifecycle analysis (Davis and Shafer, 2006; Perrotti and van Asperen, 2019). The giant ground sloth (*Eremotherium*) concept art sourced from Ugueto (2020).

Since its first discovery, the *Sporormiella* type fungi spore dominates the reconstruction of megafaunal presence and abundance. Within contemporary sites, a threshold of >2% of the total pollen assemblage (TPA) possibly represents an active abundance of megafauna (Davis and Shafer, 2006; Gill *et al.,* 2013). This threshold has been extrapolated to longer time scales to identify functional extinction events, which is when *Sporormiella* declines <2% suggesting that megafauna become so rare as to cease imposing a signal on the landscape (Davis and Shafer, 2006; Raczka *et al.,* 2018). However, the functional extinction threshold from an arid region of Western North America (Davis, 1987) is dependent on the pollen productivity of the system (Raczka *et al.,* 2016). Thus, extrapolation between environments may not be indicative, so using other quantifications in conjunction with percentage is recommended (Raper and Bush, 2009; Perrotti and van Asperen, 2019). Furthermore, other SCF can reflect the presence of megafauna (Davis, 1987; Perrotti and van Asperen, 2019). Actually, the sum of all SCF may provide the most accurate measure for analysis and enhance the interpretation of palaeoecological spore records (Johnson *et al.,* 2015; Conroy *et al.,* 2020). Despite the information provided by SCF, just three studies in South America to date have used SCF to reconstruct Pleistocene megafaunal presence (Rozas-Dávila *et al.,* 2016; Raczka *et al.,* 2018; Raczka *et al.,* 2019) (Fig. 3). This compares with at least fourteen studies in North America, a continent that lost less genera of megafauna (72%) (Barnosky *et al.,* 2004).

However, the studies in South America have relied on the percentage of *Sporormiella* as the only SCF indicative of megafaunal presence.

Figure 3. Validation map of existing spores of coprophilous fungi studies from North and South America. The mango polygon shows Colombia, the country of interest in this research. The lilac dots represent published studies and the mango dot unpublished work (Pym, 2020). Published North American sites (Davis *et al.,* 1984; Davis 1987; Robinson *et al.,* 2005; Robinson and Burney, 2008; Davis and Shafer, 2006; Gill *et al.,* 2009; Gill *et al.,* 2012; Perrotti, 2018; Conroy *et al.,* 2020) and South American sites (Rozas-Davila *et al.,* 2016; Raczka *et al.,* 2018; Raczka *et al.,* 2019). Service Layer Credits^{a}: Esri.

Research questions and objectives

The rationale of the research presented in this thesis was to contribute to the palaeoecological literature of Pleistocene megafaunal extinctions. This research presents the first investigation on the timing and ecological consequences of megafaunal declines from Monquentiva, a diverse ecosystem in the eastern Colombian Cordillera.

In accordance with this rationale, this research looked to address three questions:

(1) When did the Late Pleistocene megafaunal extinction occur in the Colombian northern tropical Andes?

(2) What was the climate, vegetation and human background of megafaunal decline?

(3) Did any ecological consequences occur that could be attributed to a megafaunal loss?

In order to answer these questions, the objectives of this study were as follows:

(1) Analyse a well-dated sedimentary record using a multi-species SCF approach to investigate megafaunal presence

(2) Assess the interpretative value of all identifiable SCF

(3) Combine the SCF record with a multi-proxy record of microscopic pollen and charcoal to evaluate the ecological consequences of megafaunal declines in the eastern Andes of Colombia

2. STUDY AREA

Pantano de Monquentiva (hereafter Monquentiva) is a peat bog that lies in the high Andean slopes of the eastern Colombian Cordillera within a ca. 4.28 ha natural park (4°54”N, 73°45”W) (Fig. 4). The site is found in the jurisdiction of the Municipality of Guatavita, Cundinamarca, roughly 50 km northeast of the city of Bogotá. Monquentiva lies in an altitudinal strip between 2900-3500 metres above sea level (hereafter masl). Despite this elevation, the site is a relatively flat ovoidal area with slopes of less than 5° (Serrano, 2019; Espinoza *et al.,* 2022). Small streams upon the eastern side of the mountain range contribute to the site's hydrology, which feeds into the Orinoco river basin (Avella-M *et al.,* 2014). During pre-Hispanic times, Monquentiva was prone to flooding and may have contained an extensive lagoon (Avella-M *et al.*, 2014; Espinoza *et al.,* 2022). However, the contemporary peatbog underwent transformations through the establishment of colonial drainage systems for livestock (Gomez and Rubio, 2003; Avella-M *et al.,* 2014; Amador and Millner, 2019). The shape and position of Monquentiva are controlled by the Río Blanco - Machetá Anticline fold and Machetá fault (Kammer *et al.,* 2020; Espinoza *et al.,* 2022) built up upon sedimentary Cretaceous rocks (Kammer *et al.,* 2020).

Monquentiva is characterised by a low 11°C average annual temperature (CAR, 2007; Rojas *et al.,* 2010). The mean annual precipitation in Monquentiva is 1425 mm, with a unimodal regime of heaviest rainfall between April and November (CAR, 2000; 2007; Avella-M *et al.,* 2014). The main climatic factors influencing Monquentiva are the annual migration of the Intertropical Convergence Zone (ITCZ) bringing moisture from the Amazon and the Atlantic Ocean and the irregular periodic variation in winds and sea surface temperatures associated with the El Niño-Southern Oscillation (ENSO) (Poveda *et al.,* 2005; Poveda *et al.,* 2006). The topography of the Andean mountain range also plays an influential role. This orographic barrier interrupts the easterly airflows from the Amazon basin forcing the air to rise, covering the slopes of the eastern Andean flank with fog (Poveda *et al.,* 2005).

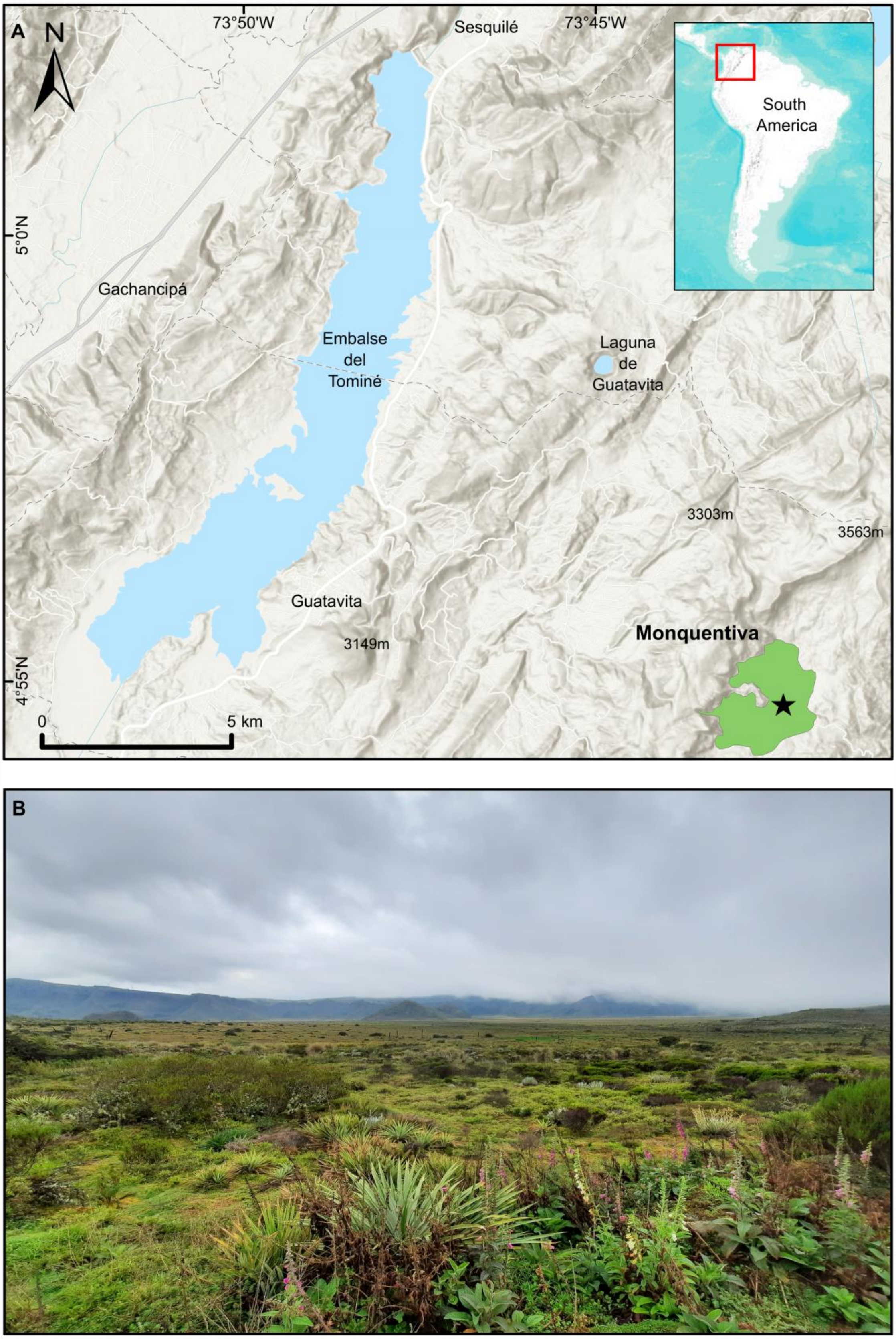

Figure 4. Location of the study site. (A) Map of Pantano de Monquentiva (green polygon), Colombia (red square). The black star shows the location of the coring site. (B) Field photograph of the Monquentiva peat bog; photo taken by Pym, 2022.

The climate, geographical location and topography of Monquentiva favour a mosaic of vegetation and concentration of biodiversity along a narrow altitudinal gradient in which the High Andean Forest, Subpáramo and Páramo are the most abundant vegetation types (Langebaek, 1985; Avella-M *et al.,* 2014; Espinoza *et al.,* 2022). High Andean forest is the most represented vegetation type surrounding Monquentiva today (76%), in which *Weinmannia* and *Clusia* dominate (Avella-M *et al.,* 2014). Other abundant arboreal genera include *Brunellia*, *Clethra*, *Drimys*, *Hedyosmum*, *Ternstroemia*, and *Vallea* (Rangel-Ch, 2000; Avella-M *et al.,* 2014). The Subpáramo follows in representation and is made up of shrubby species including *Aragoa*, *Arcytophyllum*, *Diplostephium*, *Hypericum*, *Gaultheria*, *Paepalanthus* and *Puya* (Avella-M *et al.,* 2014). The Páramo vegetation represents >20% of the flora in Monquentiva and contains a varied number of vegetation types dominated by grasses and herbs (Avella-M *et al.,* 2014). Poaceae is the largest component of the Páramo including species such as *Calamagrostis* and *Espeletia* (Rangel-Ch, 2000; Avella-M *et al.,* 2014).

Monquentiva's ecological richness and mosaic of vegetation make the site an attractive habitat for extant megafauna. This includes species of megafauna that survived the Pleistocene extinction, such as the white-tailed deer (*Odocoileus virginianus),* Brocket deer (*Mazama pita*) and Andean bear (*Tremarctos ornatus*) (Cooke, 1998; García-Rangel, 2012; Martínez-Polanco, 2019). Macrofossil evidence for extinct Pleistocene megafauna is limited in Colombia (Barnosky and Lindsey, 2010). However, skeletal records of Mastodons (*Haplomastondon)* have been dated between ca. 40,000 and 15,000 B.P in Bogotá (van der Hammen and Correal-Urrego, 1978). Megafaunal remains have also been found in Tocaima, an archaeological site at 340 masl (Correal-Urrego, 1993; Correal-Urrego, 2005; Alfonso-Rojas *et al.,* 2021). In Tocaima, massive bones of gomphotheres (*Notiomastodon platensis*) and isolated bone fragments associated with bones of giant ground sloths (*Eremotherium*) have been recovered. These findings alongside lithic artefacts associated with the genus gomphothere (*Cuvieronius* and *Stegomastodon*) recovered from Tibitó at ca. 2500 masl provides evidence for an ecosystem rich in megafauna in Bogotá during the Late-Pleistocene and the diversity of species found in Colombia (Correal-Urrego, 1981; Prado *et al.,* 2005; Borrero, 2009; Alfonso-Rojas *et al.,* 2021). However, at higher elevations such as Monquentiva, no macrofossil remains are yet reported in the literature.

3. MATERIAL AND METHODS

Core collection and sampling

A 3.65-m sediment core labelled MAR19-II was recovered from Monquentiva using a modified Livingston piston corer (Colinvaux *et al.,* 1999) in 2019. The core was transported in sealed aluminium tubes to the Tropical Palaeoecology Laboratory at the University of Exeter. Subsequently, the cores were open lengthwise and stored at 4°C. The Troels-Smith method (Kershaw, 1997) was used to describe stratigraphic units in the four 1-m core sections. Sixteen bulk sediment samples were extracted and sent to the Radiocarbon dating facility at the Queen's University Belfast for ^{14}C dating (Table 1). The intervals for ^{14}C dating were selected by visual analysis of the sediments' stratigraphic changes and to give equitable dating of the whole core. A chronological model was built using the Bacon package v.2.3.9.1 (Blaauw and Christen, 2013) within RStudio (RStudio Team, 2020) (Fig. 5).

This study focused on the upper two drives, Drive 1 (from 40-77 cm) and Drive 2 (78.1-177 cm) of the MAR19-II sediment core. Volumetric samples of 1 cm^3 were extracted for fungal spore quantification between 40 and 137.1 cm to cover the Late-Pleistocene and early-Holocene. Samples of 1 cm^3 for charcoal and 0.5 cm^3 for pollen were also extracted between 40 and 137.1 cm core depth.

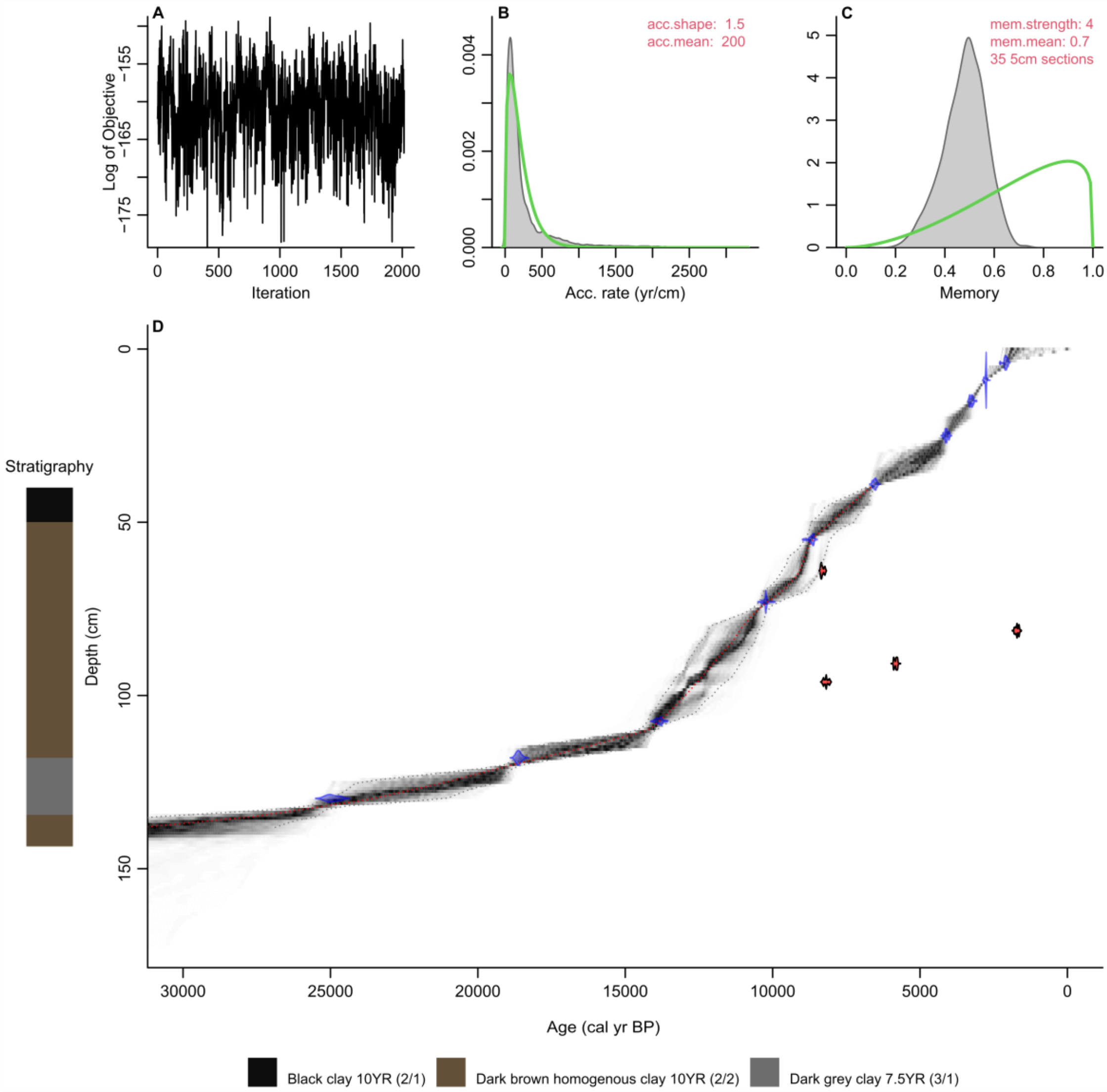

Figure 5. Bayesian age-depth model and stratigraphic descriptions for the Monquentiva core. The inset figures show the models: (A) Markov Chain Monte Carlo (MCMC) iterations; (B) distributions for the accumulation rate (Bacon MCMC iterations estimates the accumulation rate in years/cm; so more correctly, sedimentation times); (C) the memory of variability; and (D) the calibrated ^{14}C dates (transparent blue) and the age-depth model; red curve shows the 'best' model based on the weighted mean age for each depth. The filled red radiocarbon dates represent the outliers identified using Oxcal analysis (Ramsey, 2009a, b). Stratigraphic descriptions include Munsell colour notations (Munsell Colour, 1992).

Table 1: Radiocarbon ages (^{14}C) from organic lake sediments and calibrated ages (cal yr BP, IntCal20, Reimer et al., 2020) for the Monquentiva core. Calibrated ranges are rounded to the nearest 10 years.

CoreID	LabID	Drive	Depth (cm)	Description	Age (BP)	Error (±)	Age (calibrated range, 2σ)
MAR19-II	UBA-45475	1	4	Organic lake mud	2115	26	1990– 2160
	UBA-44495	1	9	Organic lake mud	2647	25	2720-2760
	UBA-45476	1	15	Organic lake mud	3047	30	3110–3380
	UBA-44496	1	25	Organic lake mud	3750	28	3890–4270
	UBA-42144	1	39	Organic lake mud	5734	36	6300–6700
	UBA-43589	1	55	Organic lake mud	7868	37	8480–9000
	UBA-44497*	1	64	Organic lake mud	7499*	37	8990-10090
	UBA-44498	1	73	Organic lake mud	9077	46	10000-10550
	UBA-45477*	2	81.3	Organic lake mud	1786*	30	10520-12100
	UBA-44499*	2	90.8	Organic lake mud	5068*	31	11120-13190
	UBA-45478*	2	96.1	Organic lake mud	7367*	40	11600-13620
	UBA-44500	2	107.4	Organic lake mud	11981	63	13300-14400
	UBA-45479	2	118	Organic lake mud	15347	69	16990–18740
	UBA-43590	2	129.7	Organic lake mud	20707	103	21090–25270
	UBA-45480	2	142.5	Organic lake mud	36818	598	30710–41500
	UBA-42145	2	162.7	Organic lake mud	42623	162.7	36310–48260

Laboratory analysis

Fungal spores were prepared following a modified version of Faegri *et al.* (1989). This modification removed acetolysis, which can cause spore deterioration (van Asperen *et al.,* 2016). A known number of exotic *Lycopodium* spores (Batch 1031; 20,848 spores/tablet) was added for SCF and pollen analysis before processing. Percentages were calculated based on the total pollen assemblage (hereafter %TPA) and the *Lycopodium* spores were used to calculate concentrations per volume (Stockmarr, 1972). SCF treatment included 10% HCl and 10% KOH, warming in a 90°C ultrasonic bath, sieving at 180 μm, density separation using sodium metatungstate $Na_6(H_2W_{12}O_{40})$ at 1.9-2.0 grams/litre and suspending in glycerol (van Asperen *et al.,* 2016). Spores and pollen were identified using a Zeiss Axioskop light microscope at 400x and 1000x magnification. All fungal spores were quantified until 300 *Lycopodium* were counted per sample (Etienne and Jouffrey-Bapicot, 2014).

The fungal spore quantification included the commonly-used *Sporormiella* taxon as well as all identifiable coprophilous, semi-coprophilous and non-coprophilous spores. The spore identification was conducted using published descriptions, fungal keys and images (van Geel *et al.,* 2003; Cugny *et al.,* 2010; Guarro *et al.,* 2012; Revelles *et al.,* 2016; Loughlin *et al.,* 2018). Where identification at the taxa level became difficult, spores were assigned to their closest morphotype (Perrotti and van Asperen, 2019; van Asperen *et al.,* 2020). Spore morphotypes were assigned to their primary substrate following existing associations (Perrotti and van Asperen, 2019; van Asperen *et al.,* 2020).

The pollen and charcoal records were used to reconstruct vegetation changes and past fire activity. Pollen and charcoal samples were prepared following their respective standard protocols (Faegri *et al.,* 1989; Whitlock and Larsen, 2002). A pollen sum of 300 pollen grains per sample were identified and counted using keys and descriptions for Andean palynology (Hooghiemstra, 1984; Colinvaux *et al.,* 1999; Bush and Weng, 2006; Velásquez *et al*., 2022) and modern reference material archived in the tropical pollen reference collection at University of Exeter. The ecological and habitat affinity of pollen taxa were extracted from the literature (e.g. van der Hammen and González, 1960; Hooghiemstra, 1984; Marchant *et al.,* 2002; Bernal *et al.,* 2019; Espinoza *et al.,* 2022). Charcoal particles were sieved to retain fragments >180 µm (macroscopic) and 106 – 63 µm (microscopic) (Whitlock and Larsen, 2002). The retained particles were manually separated and photographed using a Zeiss Stemi stereo microscope at 50x magnification. Subsequently, charcoal area and raw counts (Clark and Patterson, 1997; Halsall *et al.,* 2018) were extracted using image analysis in ImageJ software (Abràmoff *et al.,* 2004). The macroscopic fraction were extracted at a 0.8x zoom using a set calibration scale of 106 pixels/µm and the microscopic fraction at a 1.25x zoom and 170 pixels/µm calibration scale.

Qualitative and quantitative analysis

Stratigraphic diagrams of selected pollen taxa were plotted using C2 v.1.7.7 (Juggins, 2007). Confidence limits were calculated for the key spore concentration data to assess uncertainty (Maher, 1981: 179). A Pearson correlation coefficient was calculated to test correlations between key spore taxa (Johnson *et al.,* 2015) using SPSS (IBM Corp, 2020). SCF that showed positive and significant correlations were grouped to create a multi-species group of key SCF associated with megafaunal abundance (Dix and Webster, 1995; Johnson *et al.,* 2015; Perrotti and van Asperen, 2019). A sequential t-test analysis of regime shifts (STARS) (Rodionov, 2004) was performed using key SCF concentration to identify statistically significant deviations in megafaunal abundance. The analysis utilised a regime shift index (hereafter RSI) to quantify the size of the regime shift (Rodionov and Overland, 2005) and was calculated using a cut-off length $l = 4$ and probability level $p = 0.05$. STARS analysis was deployed using the Package *rshift* (Room *et al.*, 2022). Canonical correspondence analysis (CCA) (Oksanen, 2009) was performed to test the influence of constraining variables (megafaunal abundance and fire activity) on the distribution of vegetation. CCA analysis was performed on key SCF concentration, macroscopic and microscopic charcoal counts, and pollen percentages. The CCA was performed using the R package *vegan* (Oksanen *et al*, 2007), and included every pollen taxon quantified with an abundance over 1% TPA to reduce the weighting of rare taxa (Urrego *et al*., 2009; Urrego *et al.,* 2013). Both STARS and CCA were performed within RStudio (RStudio Team, 2020).

To reconstruct local fire history and identify significant fire events near Monquentiva (Clark *et al.,* 1996; Higuera *et al*., 2009), raw charcoal counts were converted into interpolated charcoal concentration (hereafter CHAR, particles/cm^3) and separated into peak magnitude and peak frequency using CharAnalysis v.1.1 within Matlab (Higuera, 2009, MathWorks, 2019). Zone division for charcoal in CharAnalysis used the whole record of samples with depth data from the youngest to oldest age (6,600–32,000 BP). CHAR values were interpolated to 200-year intervals based on rates of sediment accumulation and median sample resolution (Espinoza *et al.,* 2022). Charcoal frequency (C_{back}) was estimated using a LOWESS smoother method with a 1000-year smoothing record (Higuera, 2009; Espinoza *et al.,* 2022).

4. RESULTS

Chronology and stratigraphy

The 97.5-cm sediment section analysed provided a record of sediment accumulation from 30,290 to 6700 BP (Table 1, Fig. 5). Before age model construction, four of the sixteen-^{14}C ages were detected as outliers in Oxcal v.4.4 (Ramsey, 2009a), using the general outlier model (Ramsey, 2009b, Appendix D). These outliers were excluded from the age-depth model as they likely represented age reversals (Trachsel and Telford, 2017). The chronological model for MAR19-II (Fig. 5) used acc.shape=1.5 and acc.mean=200 as priors. The radiocarbon dates were calibrated using the IntCal20 calibration curve (Reimer *et al.,* 2020). Five samples at the top of drive 2 in the core were realigned after ^{14}C ages revealed they represented Holocene sediment. Locked pistons generally do not slip when pushed through lake muds (Colinvaux *et al*., 1999) and sediment mixing is rare. However, maintaining an efficient core seal is complex and in this case pressure may have released the rubber seal of the piston (Colinvaux *et al*., 1999; Last and Smol, 2002) and Holocene sediments were collected at the top of drive 2. In the basal part of the drive, between 143.5 and 135 cm depth (ca. 38,820-27,740 BP) the sediment is characterised by dark brown homogenous clay (Munsell colour 10YR 2/1) (Fig. 5). A sharp boundary from 135 cm is followed by a 17 cm layer of very dark grey clay (7.5YR 3/1) sediment up to 118 cm (ca. 17,900 BP). From 118 to 92.5 cm depth (17,900-12,350 BP) the sediments returned to a dark brown homogenous clay (Munsell colour 10YR 2/2). This section is overlain at the top of drive 2 with a layer of black homogenous clays (10YR 2/1) that extends to 50 cm depth (ca. 8080 BP) in MAR19-II drive 1.

Spores of coprophilous fungi (SCF) pollen and charcoal records

The SCF record was composed of 28 identifiable taxa, including eight key SCF (Fig. 6). SCF were found preserved in 36 of the 52 subsamples analysed (van Geel *et al*., 2007). In total, 1062 fungal spores were counted, with an average of 20 spores per sample (minimum 0; maximum 118). Confidence intervals calculated for key SCF concentrations showed that the uncertainties attributable to count size were minimal as the intervals are narrow (Fig. 7), this suggested the sampling effort was sufficient to provide statistical validity to the key spore data (Maher *et al.,* 2012). The SCF and pollen record was divided into five palynological zones based on changes in the core stratigraphy, key SCF regime shifts, and prominent changes in SCF and pollen assemblages (Fig. 7 and see Appendix A for complete pollen record). This includes zone M5, a chronologically floating zone dating between ca. 2,150 and 1,170 BP. Charcoal counts and area showed no observable differences in the Late Holocene ca. 2150 - 1170 BP (Appendix B). The CHAR concentration, peak magnitude and frequency of fires in Monquentiva were greater in the Early to Mid-Holocene samples (Fig. 8). CHAR analysis could not be run on the charcoal data from zone M5 due to the low number of samples.

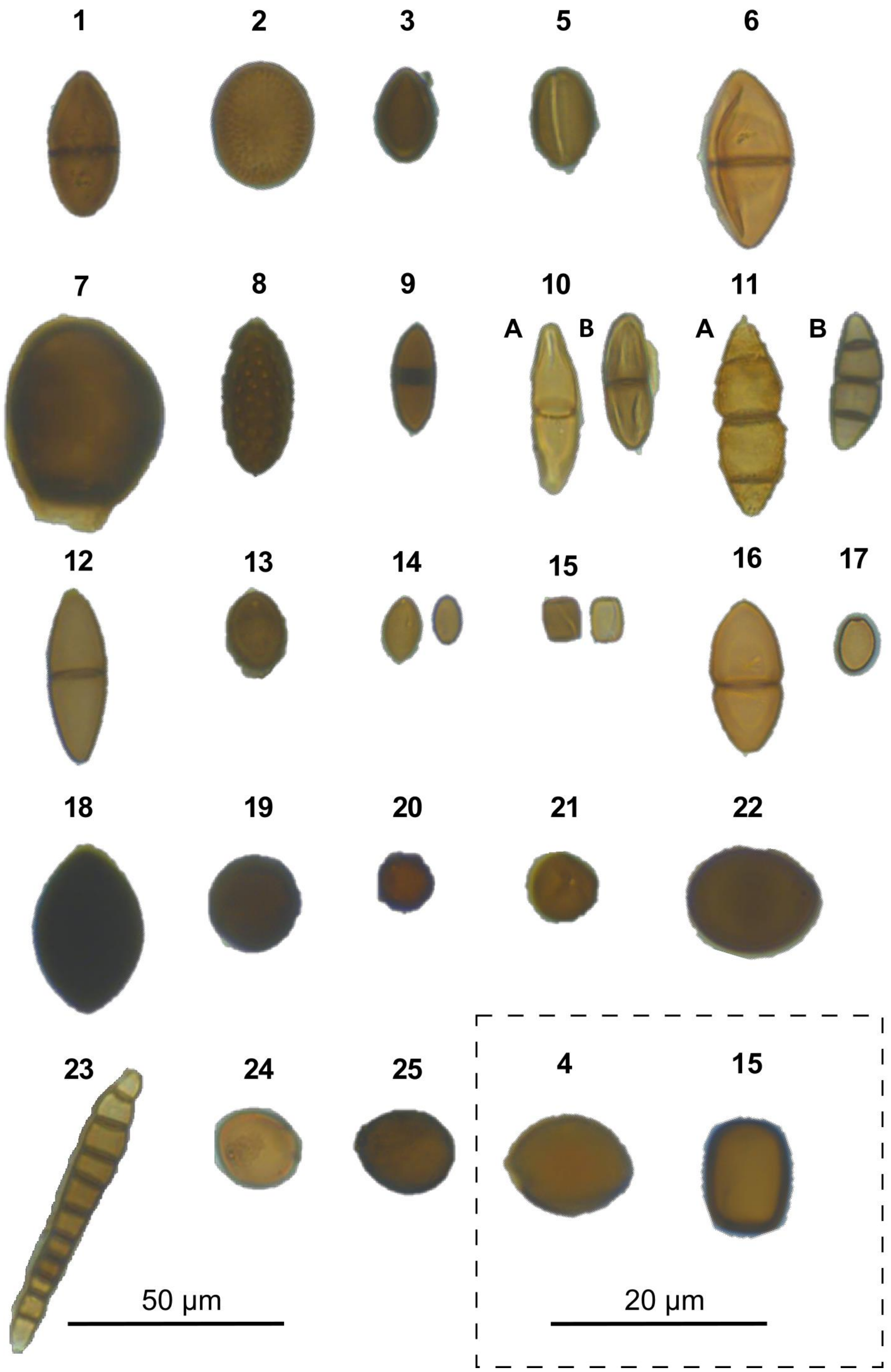

Figure 6. Identifiable fungal spore morphotypes recovered from the Monquentiva record. Due to its size, morphotype 4 (*Chaetomium*) is photographed at 1000-x magnification. Three taxa were not included in the figure due to image quality. *Sporormiella* (morphotype 15) is photographed at both magnifications. 1, *Arnium imitans* (*A.imitans)*; 2, *Achaetomium*; 3, *Cercophora*; 4, *Chaetomium*; 5, *Coniochaeta*; 6, *Delitschia*; 7, *Endophragmiella*; 8, *Gelasinospora*-types; 9, 0U-5; 10, 0U-18 AFF; 11, OU-100 AFF; 12, OU-108; 13, *Podospora*; 14, *Sordaria*. 15, *Sporormiella*; 16, *Trichodelitschia*; 17, UAB-1; 18, UAB-2; 19, UAB-7; 20, UAB-15; 21, UAB-30A; 22, UAB-32; 23, UAB-40; 24, UAB-48; 25, UAB-50. Morphotypes OU- and UAB- identified using keys from Loughin *et al*. (2018) and Revelles *et al*. (2016).

Zone M1 (30,300-22,900 BP)

In this zone, the highest abundance of SCF was observed (Fig. 7). *Sporormiella* peaked at 417 spores/cm^3 (< 1%), *Sordaria* at 1737 spores/cm^3 (3%), and *Podospora* at 139 spores/cm^3 (< 1%). The record of key SCF also included *Arnium imitans* (1946 spores/cm^{3,} 3%), *Coniochaeta* (695 spores/cm^3, 1%), *Delitschia* (208 spores/cm^3, < 1%) and *Cercophora* (139 spores/cm^3, < 1%). The most abundant pollen taxa were Poaceae (49%), Asteraceae (16%) and *Alnus* (15%) (Fig. 7). Other prominent tree and shrub taxa occurring at < 5% are *Hedyosmum*, *Hypericum*, Melastomataceae, *Podocarpus* and *Weinmannia*. Before 25,000 BP, macroscopic and microscopic charcoal concentrations were low (<20 particles/cm^3), but increased to 91 and 157 particles/cm^3, respectively at ca. 24,240 BP (Fig. 8). Peak frequency for both charcoal fractions remained below <2 fires per 1000 yr. The STARS analysis identified a key SCF regime shift at 24,240 BP reaching 2.3 RSI (Fig. 7).

Zone M2 (22,900-17,890 BP)

Zone M2 is characterised by the near absence of SCF (Fig. 7). OU-100 and UAB-2 were the only fungal spores recovered ca. 19,900 and 17,890 BP (69 spores/cm^3) (Appendix C). Asteraceae (36%) and *Alnus* (25%) were the most abundant pollen taxa, while Poaceae remained relatively low (20%) (Fig. 7). *Hedyosmum* (4%), *Podocarpus* (4%), *Valeriana* (2%) and *Weinmannia* (1%) were all present. Arboreal taxa such as *Morella* and *Myrsine* increased slightly (1-2%). Macroscopic (<2 particles/cm^3) and microscopic (0-29 particles/cm^3) charcoal remained low (Fig. 8). Peak frequency for both charcoal fractions increased in this zone (between 0 and 2.5 fires per 1000 yr). One key SCF regime shift was detected in the zone, reaching 1.23 RSI at 17,890 BP (Fig. 7).

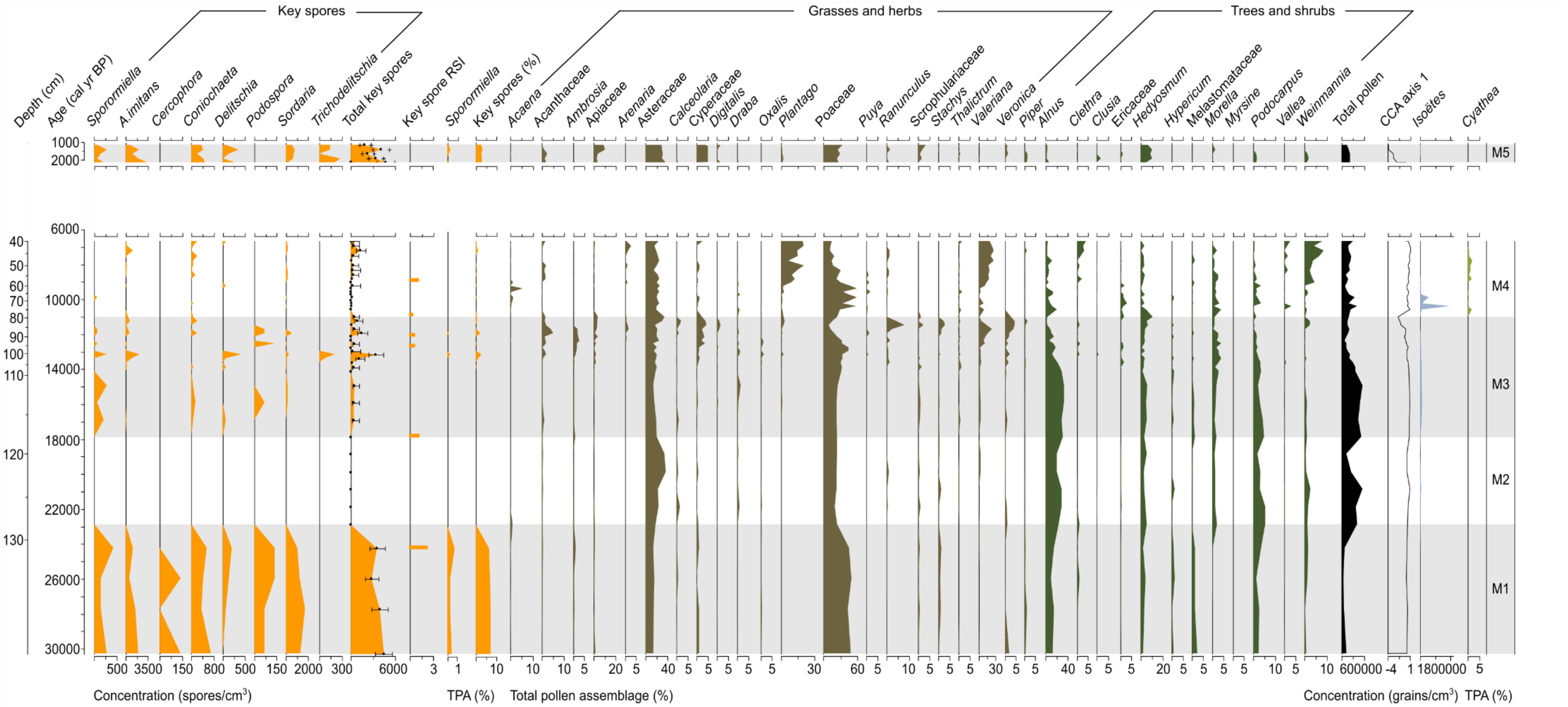

Figure 7. Summary diagram of the most abundant spore and pollen taxa recorded from the sediments of Monquentiva. All spores are expressed as a concentration per cubic centimetre (spores/cm^3). Key SCF concentration shows the 0.95 confidence interval (Maher, 1981). The key SCF RSI shows the regime shift analysis and plots the statistically significant shifts in key SCF concentration.

Zone M3 (17,890-10,990 BP)

In zone M3 SCF rebounded to levels comparable to those recorded in zone M1 (Fig. 7). Key SCF concentration fluctuated between 0 and 2154 spores/cm^3 (0-3%). *Sporormiella* increased within this zone (278 spores/cm^3, < 1%), along with *Arnium imitans* (3336 spores/cm^3, 2%), *Delitschia* (416 spores/cm^3, < 1%) and *Sordaria* (695 spores/cm^3, < 1%). *Podospora* (139 spores/cm^3, <1%), *Coniochaeta* (208 spores/cm^3, <1%) and *Trichodelitshia* (208 spores/cm^3, < 1%) were also present. Herbaceous taxa such as Asteraceae (20%) and Poaceae (27%) dominated in this zone (Fig. 7). Acanthaceae (1-5%)*, Ambrosia* (0-3%)*,* Apiaceae (0-4%)*,* Cyperaceae (0-4%), *Draba* (0-2%)*, Ranunculus* (0-8%) and *Valeriana* (0-24%) all increased in abundance. *Alnus* (29%) and *Podocarpus* (4%) increased again up to ca. 14,150 BP before declining to 2% and 0% respectively by 10,990 BP. *Hedyosmum* (4%) and Melastomataceae (1%) were present whilst Ericaceae (0-2%) and *Morella (*1-4%) increased. Macroscopic charcoal was absent at 17,890 BP but increased to 59 particles/cm^3 by 11,200 BP alongside the largest macroscopic charcoal peak recorded (25 particles/cm^{-2} peak^{-1}) (Fig. 8). Peak frequency steadily increased (from 2 to 3 fires per 1000 yr). Microscopic charcoal increased from 0-65 particles/cm^3 across the zone. By 14,200 BP microscopic peak frequency decreased to <1 fires per 1000 yr before rising to >3 fires per 1000 yr by 12,000 BP. The regime shift analysis recorded two key SCF changes at 12,770 and 12,140 BP (0.681 and 0.621 RSI) (Fig. 7).

Zone M4 (10,990-6700 BP)

Zone M4 showed a reduction of all SCF (Fig. 7). Between 11,915 and 9720 BP, key SCF declined from 1459 to 0 spores/cm^3 (2-0%). *Sporormiella* was found in only one sample at 9890 BP whilst *Cercophora*, *Podospora* and *Trichodeltischia* were absent. At ca. 7220 BP, *Arnium imitans* (1112 spores/cm^3, 1%) and *Sordaria (*139 spores/cm^3, < 1%) increased, aligning with a rise in key SCF to 1251 spores/cm^3 (> 1%). Most grasses and herbs declined at the onset of this zone including Cyperaceae (2-0%), Acanthaceae (2-0%), *Ambrosia* (2-0%), Apiaceae (4-0%), *Ranunculus* (8-0%), *Stachys* (3-0%) and *Veronica* (3-0%) (Fig. 7). Poaceae increased up to 59% and then decreased to 15% by 6700 BP. Asteraceae remained abundant (22%) whilst *Acaena* (0-6%), *Plantago* (1-20%)

and *Valeriana* (9-27%) increased. Tree taxa such as *Alnus* (20-0%), *Hedyosmum* (5-0%) and *Podocarpus* (4-0%) decreased in the zone, whilst *Clethra* (0-4%), Ericaceae (1-3%), *Vallea* (0-3%) and *Weinmannia* (1-8%) increased. *Cyathea* (2%) was recorded for the first time at ca. 10,600 BP. This zone displayed the highest macroscopic charcoal concentration (123 particles/cm^3) in the record ca. 10,990 BP (Fig. 8). Macroscopic charcoal peak frequency continued to increase across the zone (2.5-3.5 fires per 1000 yr). Microscopic charcoal and peak magnitude were highest in abundance reaching 190 particles/cm^3 and 123 particles cm^{-2} peak^{-1} (ca. 10,990 BP). Between 9600-6600 BP, microscopic charcoal frequency increased then decreased from 3.5-1.4 fires per 1000 yr. The interval recorded two final key SCF regime shifts at 10,990 and 9018 BP reaching 0.41 and 1.1 RSI, respectively.

Zone M5 (2150-1150 BP)

Key SCF peaked at 4726 spores/cm^3 (3%) ca. 2150 BP in zone M5 (Fig. 7). *Sporormiella* (278 spores/cm^3, < 1%), *Arnium imitans* (3405 spores/cm^3, 2%), *Coniochaeta* (487 spores/cm^3, < 1%), *Delitshia* (347 spores/cm^3, < 1%), *Sordaria* (695 spores/cm^3, < 1%), and *Trichodelitschia* (278 spores/cm^3, < 1%) were all present. Herbaceous taxa including Apiaceae (10%), Asteraceae (36%), Cyperaceae (6%), and Poaceae (34%) dominated the zone and were accompanied by Acanthaceae (< 3%), Scrophulariaceae (< 4%) and *Veronica* (< 2%) (Fig. 7). From the arboreal record, *Alnus* (3%) and *Hedyosmum* (8%) were the most representative. In this zone, *Rumex* appeared for the first time (1%) (Appendix A). Concentrations of both macroscopic (624-1308 particles/cm^3) and microscopic (1484-3574 particles/cm^3) charcoal were the highest in the record (Appendix B).

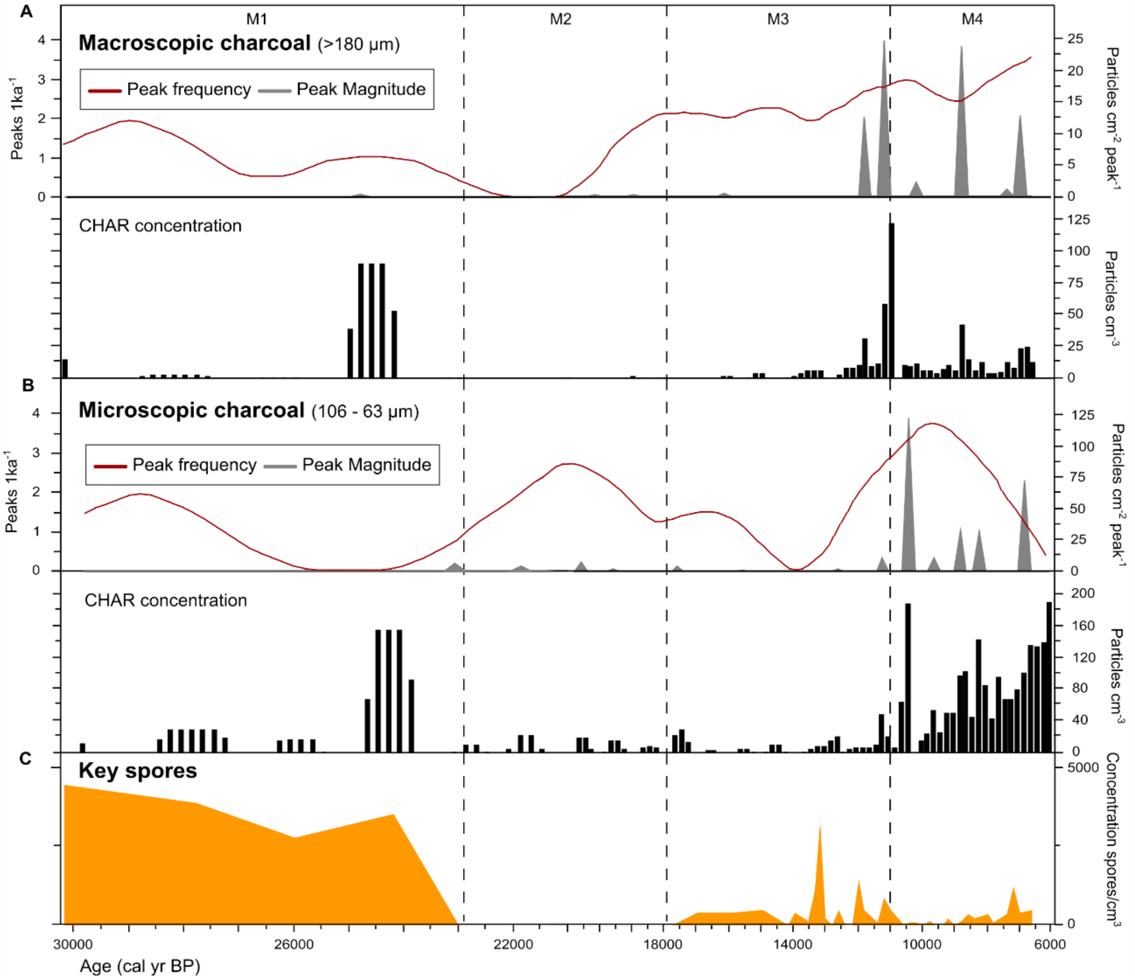

Figure 8. Monquentiva charcoal record and concentration of key spores of coprophilous fungi (key SCF). (A) Macroscopic charcoal; (B) microscopic charcoal; and (C) key SCF record. Charcoal concentration (black bars; particles/cm^3), peak frequency (red line, left hand axis; peaks/ka), and peak magnitude (grey silhouettes, right hand axis; particles/cm^2/peak) for charcoal data analysed in CharAnalysis using a LOWESS smoother model (Higuera et al., 2009). Vertical dashed lines show the four palynological zones (M1–M4) based on sedimentological changes in the core stratigraphy, key SCF regime shifts, and prominent changes in SCF and pollen assemblages as in Figure 7.

Fungal spore correlations

Sporormiella abundance in the Monquentiva record correlates positively with *A. imitans, Delitschia, Podospora, Sordaria, and Trichodelitschia* (p-value < 0.01) and with *Cercophora* and *Coniochaeta* (p-value < 0.05) (Table 2). This includes a high positive correlation between *Sporormiella* spores with *Sordaria* ($R^2 = 0.633$, $p = 0.001$), *A.imitans* ($R^2 = 0.644$, $p = 0.001$) and *Delitschia* ($R^2 = 0.691$, $p = 0.001$). Twenty other spores were recorded at Monquentiva and included 13 spores described relatively recently in the literature (Fig. 6) (Revelles *et al.,* 2016; Loughlin *et al.,* 2018). *Sporormiella* was positively correlated with three of these newly described spores OU-5 ($R^2 = 0.624$, $p = 0.001$), OU-100 ($R^2 = 0.770$, $p = 0.001$) and OU-108 ($R^2 = 0.549$, $p = 0.001$), but showed no significant correlation with OU-18, UAB-1, UAB-2, UAB-7, UAB-15, UAB-30A, UAB-32, UAB-40, UAB-48 and UAB-49 at the 0.01 level of significance (Appendix E). The significant correlations between *Sporormiella* and the other SCF were used to support the key SCF sum to represent megafaunal abundance changes over time (Fig. 7).

Table 2. Pearson correlations analysis amongst key spores of coprophilous fungi (Key SCF) from the Monquentiva record. Statistical significance of correlations are highlighted at p-value 0.01 (**) and 0.05 (*) levels.

Monquentiva	**Key SCF**						
	Sporormiella	*A.imitans*	*Cercophora*	*Coniochaeta*	*Delitschia*	*Podospora*	*Sordaria*
A.imitans	.644**						
Cercophora	.312*	.225					
Coniochaeta	.672*	.714**	.530**				
Delitschia	.691**	.722**	.069	.435**			
Podospora	.468**	.176	.485**	.462**	.138		
Sordaria	.633**	.574**	.562**	.797**	.392**	.586**	
Trichodelitschia	.364**	.749**	-.067	.402**	.605**	-.133	.206

Multivariate ordinations

The CCA analysis of the fossil pollen record grouped taxa along two axes which explained a cumulative 87% of the total variance in the dataset (Fig. 9). CCA Axis 1 explained 63% of the variance (eigenvalue: 0.0879) of pollen data, and CCA Axis 2 explained 24% of variance (eigenvalue: 0.0337). CCA Axis 1 ordinated taxa including *Ilex*, *Croton*, Gesneriaceae, and *Oxalis* at the positive end, and *Rumex*, *Alternanthera*, *Aragoa*, and Apiaceae at the negative end (Fig.

9a). The pollen taxa with the highest scores in Axis 2 were *Alternanthera*, *Rumex*, *Vicia* and *Dodonaea* at the positive extreme of the Axis, and *Carex*, *Escallonia*, Myrtaceae and Rosaceae were distributed at the negative end. The CCA ordination displayed a clear separation between samples from the Holocene at the positive extreme of Axis 2 and the Pleistocene at the negative end (Fig. 9b). Pollen from taxa found in the centre of the ordination such as Asteraceae, Poaceae, *Alnus*, *Hedyosmum* and *Podocapus* are more constant throughout the record thus are not strongly grouped to any of the environmental variables. The CCA also showed that the key SCF covaried with the negative end of Axis 2 and explained 74% of the variance along this axis. Macroscopic and microscopic charcoal covaried with the negative end of Axis 1 and both explained 98% of the variance along Axis 1.

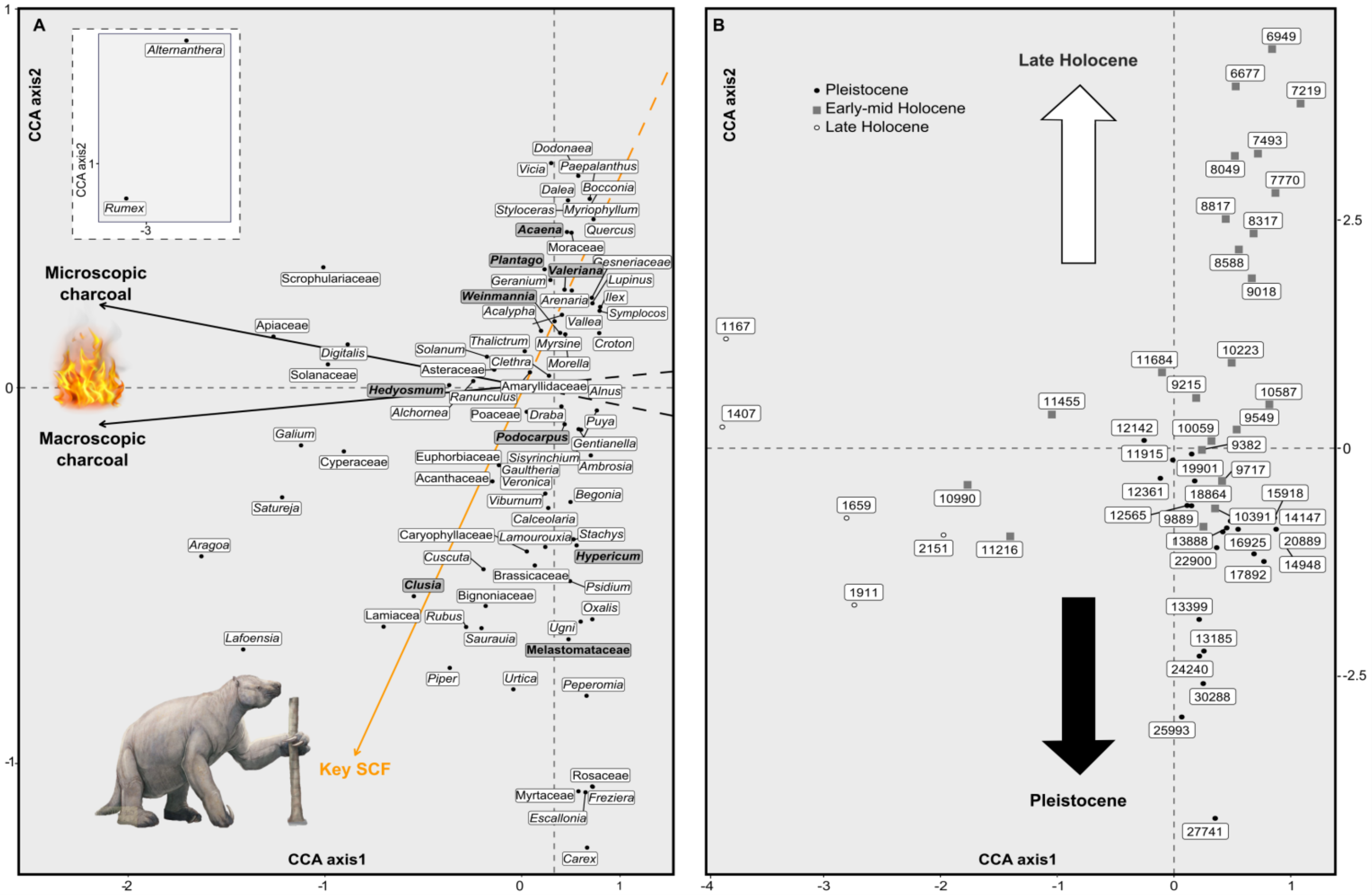

Figure 9. Canonical correspondence analysis (CCA) results for the pollen, charcoal, and spores of coprophilous fungi records from Monquentiva. (A) Species scores for the pollen record of taxa >1% the total pollen sum, using key SCF and macroscopic and microscopic charcoal as constraining variables. Bold taxa in grey boxes are discussed in detail in the text. The inset shows pollen species with high CCA Axis 1 and Axis 2 scores. The giant ground sloth (*Eremotherium*) concept art sourced from Ugueto (2020). (B) Sample scores labelled with their corresponding ages in calibrated years before present (BP).

5. DISCUSSION

The timing of megafaunal decline in the northern tropical Andes

We found robust evidence for megafaunal presence and its decline at Monquentiva (Table 2, Fig. 7). In our record, *Sporormiella* remained below the 2% functional megafaunal extinction threshold as proposed from an arid region of western North America (Davis and Shafer, 2006). However, that threshold may be inappropriate for other environments (Perrotti and van Asperen, 2019). *Sporormiella* percentages below 2% are not uncommon in the literature (e.g. Burney *et al.,* 2003*;* Perrotti, 2018). The use of *Sporormiella* concentrations (Perrotti, 2018; Chepstow-Lusty *et al.,* 2019; Conroy *et al.,* 2020) instead of percentages, has been shown to be effective to infer megafaunal extinctions (Johnson *et al.,* 2015; Raczka *et al.,* 2018; Raczka *et al.,* 2019). In lakes located in southeastern Brazilian, *Sporormiella* concentrations between 0 and 339 spores/cm^3 have indicated low to medium contemporary cattle presence around the lakes (Raczka *et al.,* 2016). We recovered *Sporormiella* at concentrations between 0 and 417 spores/cm^3, falling in the upper-end of those ranges and suggesting Pleistocene megafaunal presence. We also found statistically significant positive correlations between *Sporormiella* abundance and the other key SCF (Table 2). This allowed us to create a multi-species key SCF group to estimate megafaunal presence and track megafaunal declines (Fig. 7) (Conroy *et al.,* 2020). We combine the concentration of key SCF and statistically-significant regime shifts to identify megafaunal declines in Monquentiva.

The recovery of SCF can also be influenced by biotic and abiotic conditions related to fungal spore germination and growth. Dung fungi face interspecific competition (Kuthubutheen and Webster, 1986; Dix and Webster, 1995) and have genus- or species-specific responses to micro-environmental factors including temperature and limnological conditions (Dickinson and Underhay, 1977; Krug *et al.,* 2004). Our understanding of the role of environmental conditions on fungal spore germination is focussed on temperature zones (Lee *et al.,* 2022). However, fluctuating water levels have been shown to skew *Sporormiella* (Raper and Bush, 2009; Raczka *et al.,* 2016) and other spore records (Ponel *et al.,* 2011). This can increase or decrease the transportation and accumulation of spores in lakes (Raper and Bush, 2009;

Etienne *et al.,* 2013; Lee *et al.,* 2022). At Monquentiva, we used multi-species key SCF concentration declines to minimise the effects of environmental conditions on individual SCF germination and growth experienced by individual SCF. We also used our pollen record to infer environmental conditions such as water levels during periods of low spore concentrations to infer the presence and declines of megafauna.

The multi-species key SCF record indicates the presence of megafauna in Monquentiva and the eastern Colombian Cordillera since at least 30,290 BP (Fig. 7). Existing evidence of megafaunal presence in the tropical Andes has been derived from macrofossil remains and spore records. Megafauna macrofossil remains are scarce (Barnosky and Lindsey, 2010) but have been dated in Venezuela back to 47,990 BP (Jull *et al.,* 2004), Ecuador back to 20,980 BP (Coltorti *et al.,* 1998), Peru back to 10,150 BP (Marshall *et al.,* 1984) and Brazil back to 20,060 BP (Neves and Piló, 2003). The limited spore records produced to date provide evidence for megafaunal presence in Ecuador back to 12,000 BP (Raczka *et al.,* 2019), Peru back to 25,000 BP (Rozas-Dávila *et al.,* 2016) and Brazil back to 23,000 BP (Raczka *et al.,* 2018). In Colombia, macrofossil remains have been dated back to 40,000 BP (van der Hammen and Correal-Urrego, 1978) and although limited (Barnosky and Lindsey, 2010) have been found in Tocaima, an archaeological site at 340 masl (Correal-Urrego, 1993; Correal-Urrego, 2005; Alfonso-Rojas *et al.,* 2021) and at Tibitó at 2500 masl (Correal-Urrego, 1981; Borrero, 2009). Megafaunal presence have also been inferred from rock shelter cave paintings from Serranía de la Lindosa (ca. 500 km from Monquentiva) that date back to ca. 12,600 BP (Bischler and Pinto, 1959; Correal *et al.,* 1990). However, this evidence has been highly criticised (Baena *et al.,* 2004). Our SCF record reveals that megafauna also roamed the higher altitudes of Colombia during the Pleistocene and were present at Monquentiva and the Colombian Andes dating back to at least 30,290 BP.

Our data indicated the first wave of megafaunal decline in Monquentiva at 22,900 BP, followed by a recovery ca. 16,900 BP and a second decline by ca. 10,990 BP (Fig. 7). Such SCF fluctuations could also result from differential preservation due to water level changes (Wood and Wilmshurst, 2013; Raczka *et al.,* 2019) and water-body size (Raper and Bush, 2009; Lee *et al.,* 2022). However, the pollen record shows that *Isoëtes* was low during the onset of both megafaunal declines and did not coincide with changes in SCF (Fig. 7). *Isoëtes* is an aquatic taxon, common at the bottom of lakes, marshes and bogs in the high Páramo (van der Hammen and Gonzalez, 1960). *Isoëtes* did increase in the Monquentiva record suggesting the formation of a small water body, but ca. 600 years after the second SCF decline. Consistently low water levels and independence of the SCF and *Isoëtes* records at Monquentiva suggest the SCF concentration decreases are representative of megafaunal declines and are not due to water-level fluctuations.

The first megafaunal decline at ca. 22,900 BP was identified as a statistically significant regime shift in Monquentiva (Fig. 7). Three further key SCF regime shifts were identified at ca. 12,770, 12,140 and 10,990 BP. The shifts at 12,140 and 10,900 BP are linked to a decline in key SCF concentration from 1459 to 0 spores/cm^3. We interpret these shifts as the local extinction of some Pleistocene megafauna at Monquentiva. This record is consistent with a two-wave megafaunal decline from Lake Pacucha in the high Andes of Peru (Rozas-Dávila *et al.,* 2016). However, at Pacucha the first megafaunal decline started at 21,000 BP and resulted in an extinction by 15,800 BP (Rozas-Dávila *et al.,* 2016). In Ecuador the extinction of Pleistocene megafauna is recorded at 12,800 BP (Nascimento *et al.,* 2020) while in Lagoa Santa, Brazil is reached by 12,000 BP and recorded no megafaunal recovery (Raczka *et al.,* 2018). At Monquentiva and the Colombian Andes the second decline of megafauna (ca. 10,990 BP) was recorded later than other South American sites. However, macrofossil remains from species such as *Doedicurus* have been dated as late as 6560 BP in Argentina (Borrero *et al.,* 1998). Ecosystems are complex and highly-diverse across South America and this heterogeneity could be linked to variability in megafaunal extinction timings (Gill *et al.,* 2009; 2012; Rozas-Dávila *et al.,* 2016). Thus, we suggest that continent-wide assessments could overwrite this variability and the complexity of factors that shaped these habitats after the Pleistocene megafaunal extinctions.

Climate, vegetation and human backdrop of megafaunal declines

Páramo vegetation dominated Monquentiva between 30,000 to 22,900 BP (Fig. 10). The dominance of Poaceae up to 24,240 BP, the low abundance of arboreal elements and low total pollen concentration at Monquentiva indicated a cool and dry climate. The tree line, defined as the upper altitudinal boundary of continuous forests (Urrego *et al.,* 2011a), was lowered and open vegetation was found not just at Monquentiva but also across the high elevations in the eastern Colombian Andes (van Geel and Van der Hammen, 1973). This period corresponded with the coldest phase of the Last Glacial period (van der Hammen, 1974, Bogotá-A *et al.,* 2011). High concentrations of key SCF during the Last Glacial period at Monquentiva indicate that the open vegetation structure was favourable for megafaunal presence. Between 25,000 and 24,200 BP, CHAR increased but the charcoal magnitude and frequency remained low suggesting a period of high-intensity but low-frequency fires (Fig. 8). These high-intensity fires resulted from relatively dry conditions indicated by the low abundance of aquatic and wetland taxa including *Isoëtes* and Cyperaceae (Fig. 7). However, fire activity was not sustained during the first wave of megafaunal decline ca. 22,900 BP. This could result from the cold and dry climate at the end of the Late Glacial (Bogotá-A *et al.,* 2011; Urrego *et al.,* 2011b) and a reduction in fuel-load by the decline of Poaceae from 24,240 BP (Fig. 7).

The first wave of megafaunal decline at 22,900 BP took place during a relative glacial temperature and humidity increase at Monquentiva as evidenced by displacements of Páramo by SubPáramo vegetation and increases in arboreal elements (Fig. 7 and 7). The increase of Andean forest taxa including *Alnus* and *Podocarpus* indicated a relative increase in temperatures and the absence of *Isoëtes* indicated low water levels. *Alnus* and *Podocarpus* are cold tolerant and generous wind-pollinated pollen producers (anemophilous), and their high abundance could imply over-representation from lower altitudes (van der Hammen and Gonzalez, 1960; Colinvaux *et al.,* 1999). However, we suggest the forest tree line moved upwards, as *Weinmannia* and *Podocarpus* also increased, two taxa indicative of a local signal of upper montane forest in the Tropical Andes (Gomez *et al.,* 2007; Hagemans *et al.,* 2019). This relative warming was short-lived and temperatures decreased again as indicated by a further rise in

Subpáramo taxa such as Asteraceae and a decline of arboreal elements at ca. 20,890 BP. This fluctuation of the upper forest line is consistent with changes from lower altitudes of Colombia (Bogotá-A *et al.,* 2011) suggesting temperature changes as megafaunal populations declined during the Late-Pleistocene. By 16,930 BP, environmental conditions once again provided a favourable habitat for megafauna at Monquentiva.

The second wave of megafauna decline occurred at ca. 10,990 BP during the El Abra stadial (Fig. 10) (Hooghiemstra and van der Hammen, 1993). This period coincided with an increase in herbaceous, arboreal and shrub taxa from the high Andean forest and Páramo vegetation, suggesting a novel structure and transitional vegetation (see ecological consequences discussion below). Nearby vegetation records from Lake Fuquene (2580 masl, Bogotá-A *et al.*, 2011) and Cienaga del Visitador (3300 masl, van der Hammen and González, 1965) also show rises in *Alnus* and a vegetation mosaic of Andean forest, Subpáramo and Páramo species. The decline of megafauna at Monquentiva during the cool El Abra stadial contrasts with literature suggesting that megafaunal extinctions tracked warm interstadials (Cooper *et al.,* 2015), but it does point to declines occurring during periods of climate instability.

The decline of megafauna at Monquentiva from 10,990 BP also coincided with the earliest evidence of hunter-gatherers in Colombia (Fig. 10). Hunter-gatherer groups are reported since the Guantiva interstadial ca. 12,500 BP in the Bogotá highlands (2600 masl) and downslope from Monquentiva at 340 masl since 11,740 BP (van der Hammen and Correal-Urrego, 1978; Correal-Urrego, 1993; Triana-Vega *et al.,* 2019; Alfonso-Rojas *et al.,* 2021). Megafaunal extinctions have been linked to overhunting by humans worldwide (Martin and Klein, 1984; MacPhee and Sues, 1999) and suggested as a major driver of extinction in North America and Australia (Martin and Klein, 1984; Stuart, 1999; Rule *et al.,* 2012). In South America, our understanding of the role of overhunting in the decline of Pleistocene megafauna is less clear due to the paucity of records. Records from coastal Ecuador suggest a stratigraphic correlation between megafaunal remains and stone tools of suspected Holocene age (Ficcarelli *et al.,* 1997). However, megafaunal hunting by humans is not thought to have been determinant in their extinction at this site (Ficcarelli *et al.,* 1997).

The Pleistocene collapse of megafauna in Brazil occurred during a window of human occupation (Raczka *et al.,* 2018), but in Peru, megafaunal populations collapsed before human presence (Rozas-Dávila *et al.,* 2016). At Monquentiva megafaunal populations were unable to recover after 10,990 BP suggesting that a synergy between humans and climate could have contributed to their decline and absence. Overall, our record allows us to infer the timing of megafaunal decline and ecological consequences but we have little evidence to explore the cause of extinctions.

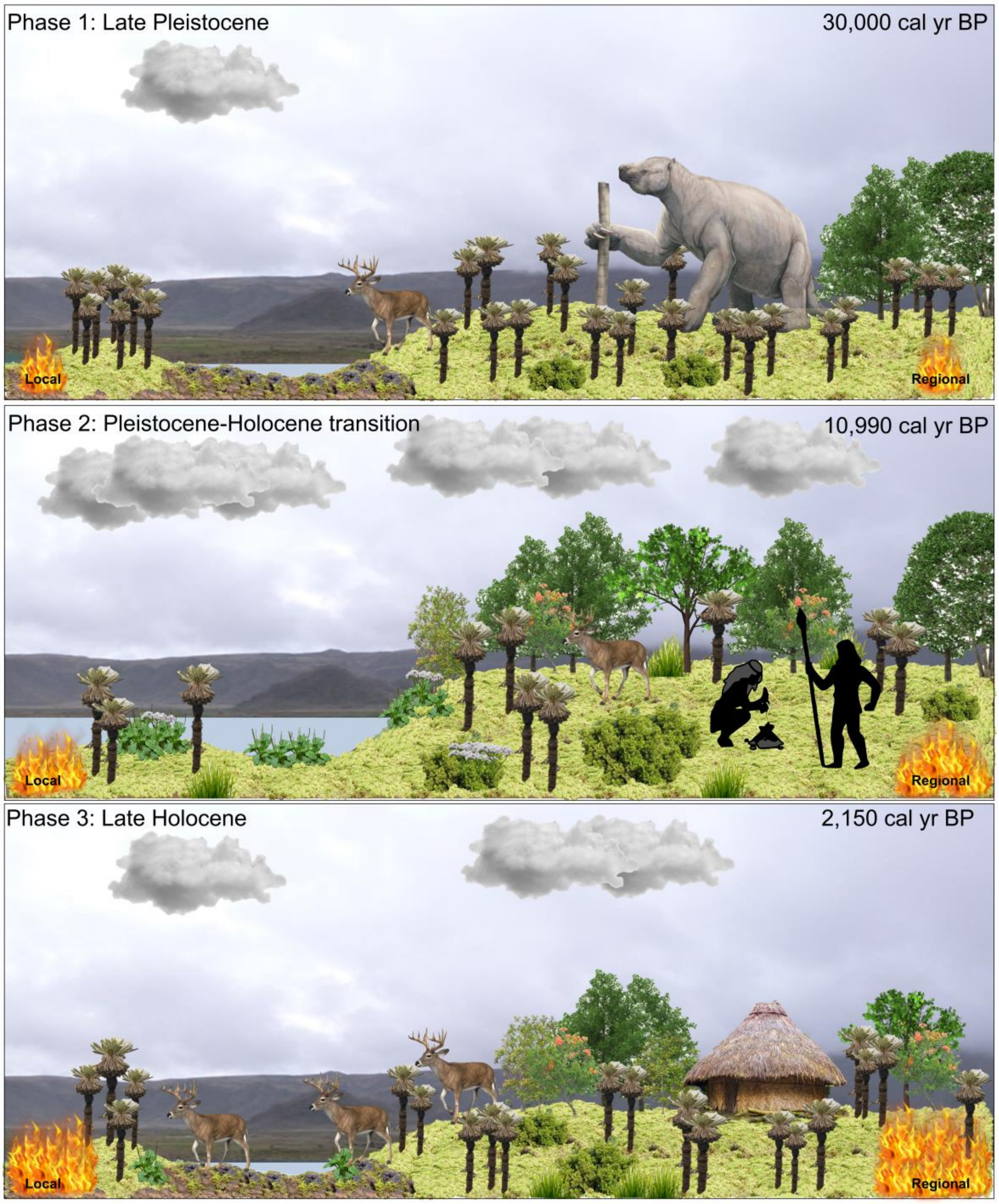

Figure 10. A conceptual landscape drawing of the changes in megafaunal presence, vegetation and fire activity reconstructed for Monquentiva during the Late Pleistocene and Holocene. Produced using Inkscape (Inkscape Project, 2022). Megafauna are depicted by the giant ground sloth (*Eremotherium*; concept art sourced from Ugueto, 2020) and a white-tailed deer representation (*Odocoileus virginianus*) (https://www.allwhitebackground.com/?p=4845; viewed 04 January 2022). The flora clipart not cited are sourced from Microsoft clipart 2016. Trees and shrubs include representations of *Alnus* and *Morella* (3d_moiler, 2014; Sharpj99, n.d.). Herbaceous taxa include *Espeletia* (Asteraceae), *Stachys* and *Valeriana* (Mergili, 2007; Vancouverislandgrows, 2018; Zwerver, n.d). Local and regional fire activity represented by relative size of flame. Silhouettes indicate hunter-gatherer groups (Vlasiuk, 2020). Kogi hut represents occupation by the pre-Hispanic indigenous group Muiscas (Benedek, 2015). Clouds and lake (blue polygon) represent humidity and lake level at the site (Garcia, 2022). Photographic backdrop of Monquentiva taken by J.W. Oughton in 2019.

Ecological consequences of megafaunal collapse

We found that some tree and shrub species became absent from the record during both waves of megafaunal decline, increasing in abundance during the partial recovery of megafauna ca. 16,930-10,990 BP (Fig. 7). Melastomataceae*, Clusia and Hypericum* all increase at Monquentiva when megafaunal abundance recovers. These pollen taxa can be dispersed by herbivores (Grabandt, 1980) suggesting a correlation that is corroborated by the CCA analysis (Fig. 9a). Across the contemporary tropics, pollination and dispersal of these families by megafauna have been recorded directly, as with the case with species of Melastomataceae, Clusiaceae, and Hypericaceae (Lemes-Martins *et al.,* 2007; Bufalo *et al.,* 2016; Escribano-Avila *et al.,* 2018). Melastomataceae and Clusiaceae are also known to be dispersed by birds (Cronquist, 1988; Sánchez-Sánchez *et al.,* 2015) however, if birds at Monquentiva dispersed species such as *Clusia* from the Clusiaceae family, we suggest this could be an indirect relation to the presence of megafauna attracting birds to the site (Galetti *et al.,* 2018). Similarly, we found that several grass and herb taxa, including Acanthaceae, Apiaceae, *Ranunculus* and *Veronica*, became absent from the record during the second wave of megafaunal decline ca. 10,990 BP (Fig. 7). This suggests that the decline of these taxa are likely a result of reduced meditation in seed-dispersal by megafauna, rather than climate alone. Such relations between seed-dispersal services and the loss of megafauna have been found in the Neotropics today where the loss of primates has led to dispersal limitation in plant species (Peres *et al.,* 2016). As Pleistocene megafauna declined in the high Andes of Peru, grasses and forbs were also observed to decline (Rozas-Dávila *et al.,* 2016). In the Brazilian lowlands, vegetation remained largely unchanged with only a few taxa declining in abundance (Raczka *et al.,* 2018). These contrasting records probably relate to differences in the original vegetation and suggest the ecological consequences of megafaunal declines were habitat-specific. In the Colombian Andes however, our palaeoecological record suggests an important role of the megafauna in the reproduction and dispersion of tree, grass and herb taxa.

The pollen record also showed palatable and woody taxa increasing at Monquentiva following the second decline of megafauna ca. 10,990 BP (Fig. 7).

Plantago is *a* highly palatable herb (Rozas-Dávila *et al.,* 2016) that increased following megafaunal declines. The CCA analysis shows that *Plantago* plotted on the opposite extreme of key spores indicating its sensitivity to megafaunal presence (Fig. 9a). *Plantago* is indicative of cold Páramo vegetation (Hooghiemstra and Flantua, 2019), thus the species representation in the record under early-Holocene warming suggests their release from megafaunal grazing. The lagged increase of *Plantago* could reflect the late-successional trait of the taxon (Hooghiemstra and Flantua, 2019). At Monquentiva, Ericaceae increases after the second megafaunal decline (Fig. 7) and plots on the opposite ecological extreme of key SCF in the CCA (Fig. 9a). Some Ericaceae are woody shrubs in Andean sites (Bush *et al.,* 2015; Rozas-Dávila *et al.,* 2016) and this increase suggests woody species overgrowth following megafaunal declines. Such woody overgrowth is also recorded in other palaeoecological records including other Andean and North American records (Gill *et al.,* 2009; 2012; Raczka *et al.,* 2018, Rozas-Dávila *et al.,* 2016). *Valeriana* declined after the second megafaunal decline but became more abundant in the Mid-Holocene when some megafaunal species recovered (Fig. 7). *Valeriana*, is also woody but commonly present in the SubPáramo-Páramo (Sylvester *et al.,* 2018; Hooghiemstra and Flantua, 2019). The first decline of *Valeriana* could thus indicate Early-Holocene warming and the Mid-Holocene rise could suggest reduced woody suppression by the reduced megafaunal populations. This is supported by the CCA analysis where *Valeriana* plots on the opposite ecological extreme of key SCF (Fig. 9a). The lack of herbivory after the second megafaunal decline probably contributed to the encroachment of palatable and woody species at the higher altitudes of the Colombian eastern Cordillera.

At Monquentiva, a turnover in arboreal taxa and reduction of an open Poaceae-dominated grassland is recorded after the second wave of megafaunal decline ca. 10,990 BP (Fig. 10). The prominent Andean taxa were Ericaceae, *Hedyosmum, Podocarpus* and *Weinmannia,* surrounded by shrubby Subpáramo grasses and herbs including *Acaena*, Asteraceae, and *Valeriana*. The presence of *Cyathea,* a tree fern that typically inhabits gaps in closed forests suggests increases in forest cover (Crystal-Arens, 2001). This ecosystem transformation at Monquentiva suggests the replacement of open vegetation with a closed formation of non-analogue vegetation following the second decline of megafauna.

This finding coincides with the consequences of defaunation reported for the Peruvian Andes (Rozas-Dávila *et al.,* 2016), other neotropical (Dantas and Pausas, 2022), and North American sites (Gill *et al.,* 2009; 2012). The flora turnover at Monquentiva occurred during the warmer Guantiva interstadial and cooler El Abra stadial 12,000-10,200 BP (Hooghiemstra and van der Hammen, 1993) thus climate oscillations could have played a role in vegetation changes observed. However, the CCA analysis showed that the abundance of some of these novel flora including *Acaena*, *Valeriana* and *Weinmannia* were ordinated on the opposite end of the constraining variable for megafauna (Fig. 9a). This suggests the transitional non-analogue vegetation was closely linked to megafaunal declines and their role in determining vegetation composition and structure at Monquentiva.

The charcoal record from Monquentiva represents a transition to higher local and regional fire activity during the early-Holocene megafaunal decline (Fig. 8). The reduction of herbivory during the early-Holocene probably led to fuel build-up of woody and grass biomass and increased fire activity. Megafaunal presence and fire activity on our CCA show an independent relationship (Fig. 9a), highlighting the link between rising fire activity and megafaunal absence. Andean megafauna likely acted as fuel-load suppressors in the tropical Andes as species including the white-tailed deer are browsers, thus trample on vegetation and feed on palatable flora (Martínez-Polanco, 2019). Our record is consistent with increased fire activity after megafaunal collapse reported in other systems after megafaunal declines (Burney *et al.,* 2003; Gill *et al.,* 2009; 2012; Rule *et al.,* 2012; Rozas-Dávila *et al.,* 2016), but it contrasts with the record from the Brazilian Cerrado where the collapse of megafaunal populations did not result in increased fire activity (Raczka *et al.,* 2018). Thus, we suggest that the complexity and diversity of South American ecosystems lead to heterogeneity and habitat specificity regarding the expected relationship between Pleistocene megafaunal decline and increasing fire activity.

Extant Holocene megafauna, climate and human activity

Monquentiva witnessed a recovery in key SCF concentrations from ca. 8800 BP (Fig. 7 and Fig. 10) that could represent the presence of extant megafauna (Perrotti, 2018; Conroy *et al.,* 2020). This probably included those that inhabit Colombian ecosystems today such as the Brocket and white-tailed deer (Cooke, 1998; Martínez-Polanco, 2019), and the Andean spectacled bear (García-Rangel, 2012). This is consistent with surveys of white-tailed deer bone remains dated back to 2320 ± 50 14C yr BP (Becerra, 1995). The recovery of megafauna under human occupation could relate to a change away from hunter-gatherer societies towards sedentism (Triana-Vega *et al.,* 2019; Archila *et al*., 2021). In the Late-Holocene, Poaceae and Asteraceae were dominant suggesting an increase in open vegetation at Monquentiva. Increases in *Hedyosmum*, *Weinmannia* and *Podocarpus* indicated an expansion of forest on the surrounding slopes (Bogotá-A *et al.,* 2011). *Rumex* appeared in the record at low but consistent percentages (Appendix A) and has been linked to degraded soils in Monquentiva (Espinoza *et al.,* 2022). The dominance of *Hedyosmum* could also suggest human disturbance and be linked to disturbed areas (Gentry, 1993). These vegetation changes could reflect disturbance by pre-Hispanic Muisca groups (Langebaek, 1985; Langebaek, 2001). Increased humidity could have resulted in a shallow water body as suggested by the rise in Cyperaceae and low abundance of *Isoëtes* (Hooghiemstra and van der Hammen, 1993). The Late-Holocene vegetation cover and environmental conditions at Monquentiva likely provided habitat, water and food for extant megafauna, allowing some species to persist in this part of the Colombian Andes until today.

During the Late-Holocene, fire activity escalated at Monquentiva (Appendix B, Fig. 10). High charcoal concentrations likely reflected increased fires linked to agriculture (Gómez *et al.,* 2007) and other anthropogenic activities (Espinoza *et al.*, 2022). Thus, the escalated fire record under Late-Holocene megafaunal presence is likely to have been induced by human activities and facilitated by climate, which coupled to overrule the suppressive effect of megafauna on the vegetation.

6. CONCLUSIONS

This study is the first in the eastern Andes of Colombia, and probably across the continent, to use a multi-species SCF record to investigate the decline of Late-Pleistocene megafauna. We showed that the combined record of coprophilous and semi-coprophilous fungi provided more robust evidence to infer megafaunal presence and declines. The multi-species SCF record from Monquentiva indicated megafaunal presence in the eastern Colombian cordillera since at least 30,290 BP. At Monquentiva, megafaunal populations declined in two waves. The first decline was reached by 22,900 BP during a relative glacial temperature and humidity increase. By 10,990 BP the second megafaunal decline was reached, a period coeval with the El Abra interstadial and the presence of hunter-gatherer groups. The extinction of some megafauna at Monquentiva also points to declines occurring during periods of climate instability. However, our data does not allow us to infer the causes of megafaunal extinctions or the potential role of overhunting.

One ecological consequence of the megafaunal declines at Monquentiva was the formation of novel vegetation assemblages. The representation of some plant species decreased whilst other palatable and woody taxa increased. This highlighted the role of megafauna in seed-dispersal and herbivory. Another ecological consequence was the increase in fire activity after megafauna declined. Pleistocene megafauna likely acted as fuel-load suppressors in the tropical Andes as they trampled on vegetation and fed on palatable flora.

Overall, we show that ecosystems in the high eastern Andes of Colombia were highly sensitive to the decline of megafaunal populations. Under the current biodiversity crisis, our understanding of the ecological consequences of megafaunal declines at Monquentiva suggest that current and future extinctions could have devastating consequences for biodiversity. This knowledge is fundamental for contemporary management and conservation efforts. To effectively manage biodiversity, these efforts must account for the effect of local herbivore declines on the dispersal of certain plant species, on fire activity and the potential loss of ecosystem services.

FUNDING

This work was supported by the BioResilience research project as a product of funding from the Natural Environment Research Council (NERC) grant number NE/R017980/1 and the Arts and Humanities Research Council (AHRC) under the Newton-Caldas ColombiaBio programme.

APPENDICES

Appendix A: Complete fossil pollen and charcoal diagram for all pollen taxa and charcoal particles recorded from the sediments of Monquentiva.

The pollen taxa are split into their ecological affinity, colour codes: Grasses and herbs (Brown-green); Trees and shrubs (Green). Malvaceae, *Salvia* and *Vicia* grouped at the end of the diagram as they can be found as trees, shrubs and herbs (Marchant *et al.,* 2002). Species are expressed as a percentage of the pollen sum (%TPA). Pollen types without visible value have an x-axis maximum of 5%. Pollen taxa unidentifiable at species level are grouped in their family and include the number of morphotypes.

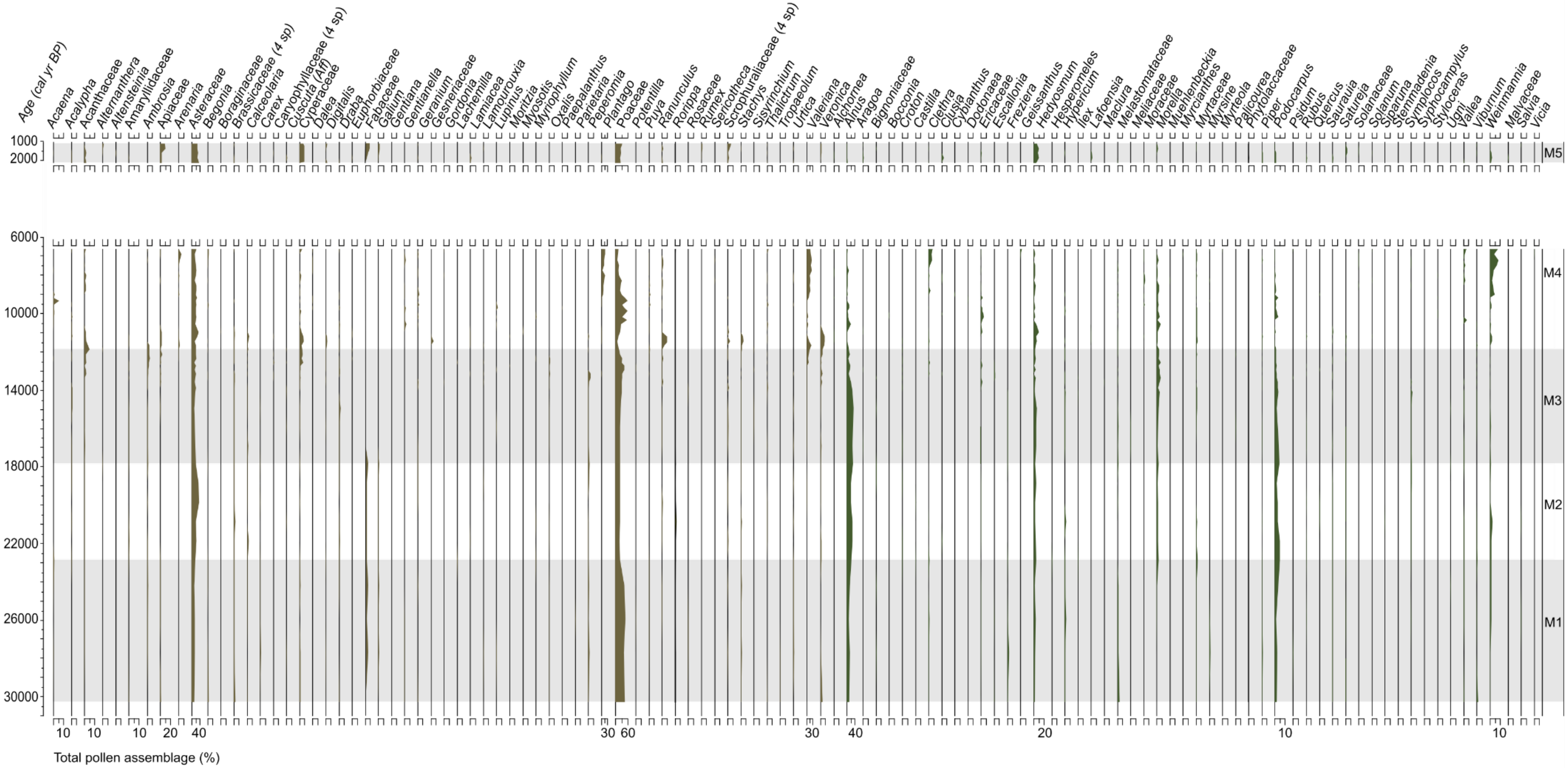

Appendix B: Macroscopic (local; black) and microscopic (regional; red) charcoal fractions. Both fractions are expressed as counts per cubic centimetre (cm³) and area (cm²/cm³). Charcoal counts in the floating Holocene samples use separate x-axis limits to the Pleistocene samples.

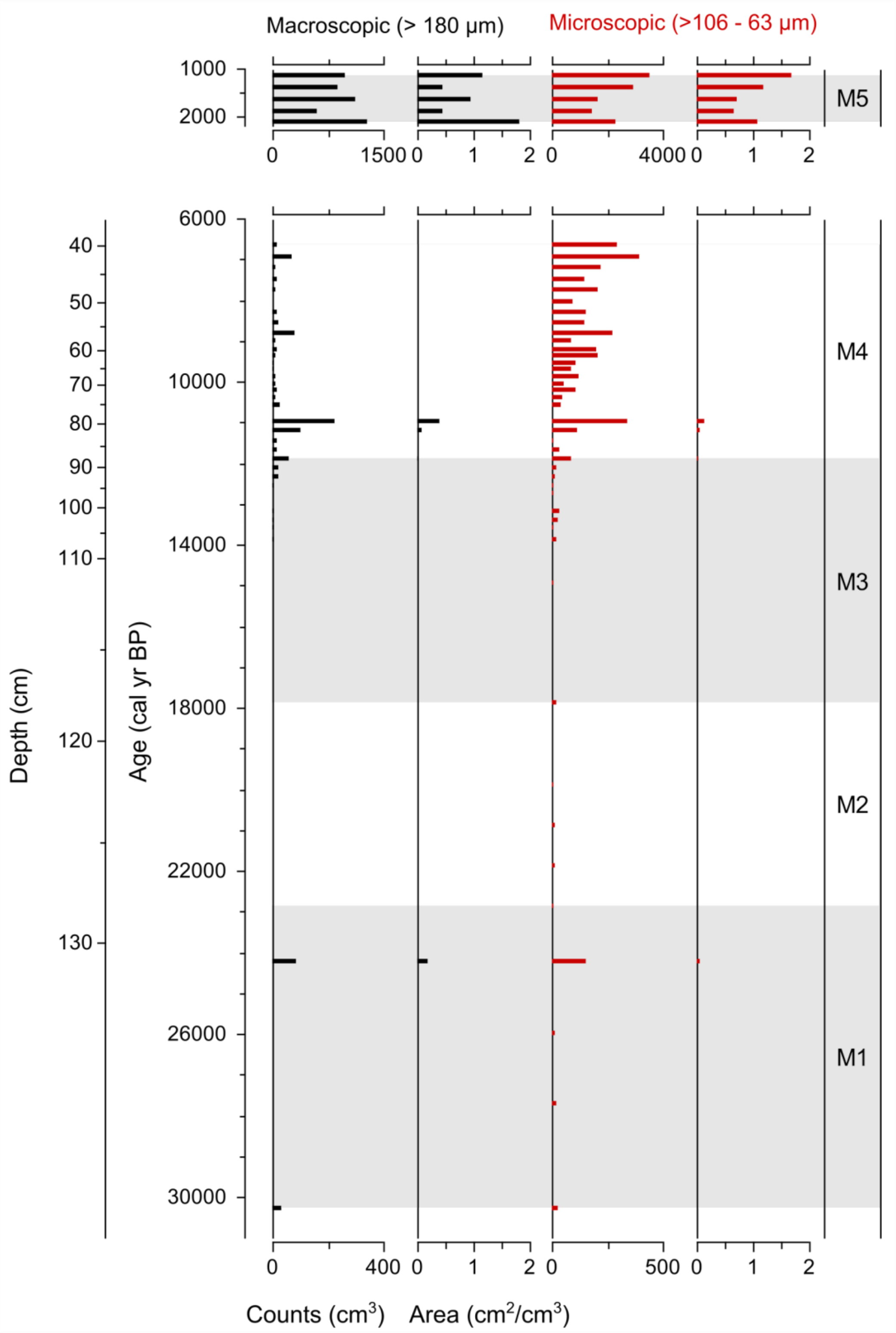

Appendix C: Complete fossil spore diagram for all identifiable fungi spore morphotypes recovered from the sediments of Monquentiva.

All coprophilous spores are expressed as a percentage of the total pollen assemblage (%TPA) and as concentration of counts per cubic centimetre (cm^3). A 1-x scale factor exaggeration is shown for all spores in the percentage quantification. Key spores (light orange) other identified fungi spores (dark orange). AFF refers to the affinity of spore morphotypes and indicates when they were assigned to their most akin morphotype.

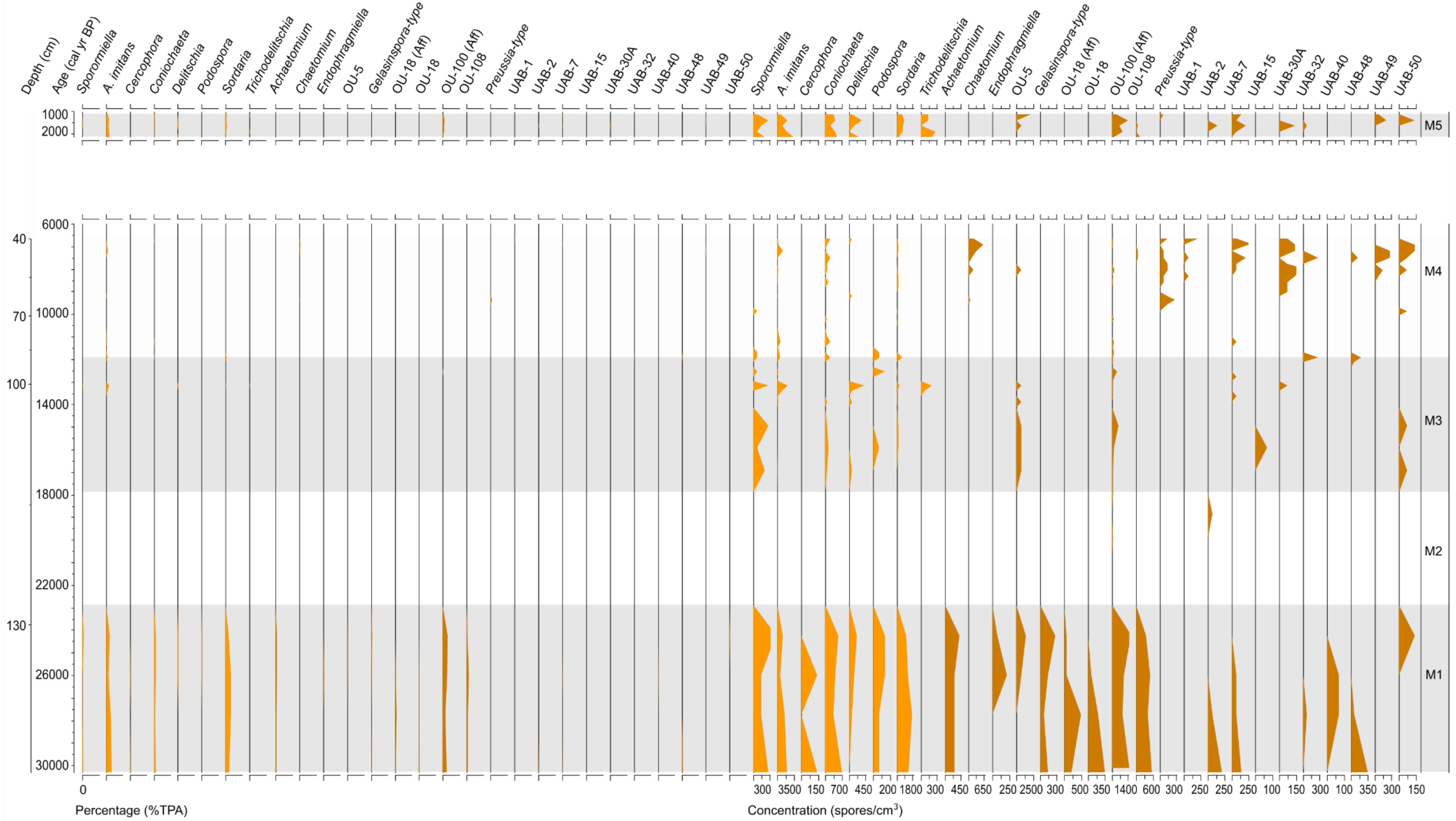

Appendix D: Adapted outputs of a general outlier model run on the Monquentiva ^{14}C radiocarbon ages, created using Oxcal v.4.4 (Ramsey, 2009a; Ramsey, 2009b).

The prior probability for each measurement being an outlier was set to 0.05. The posterior column provides the probability for each measurement being an outlier.

Colour codes: Accepted age (Blue); Likely outlier (Red).

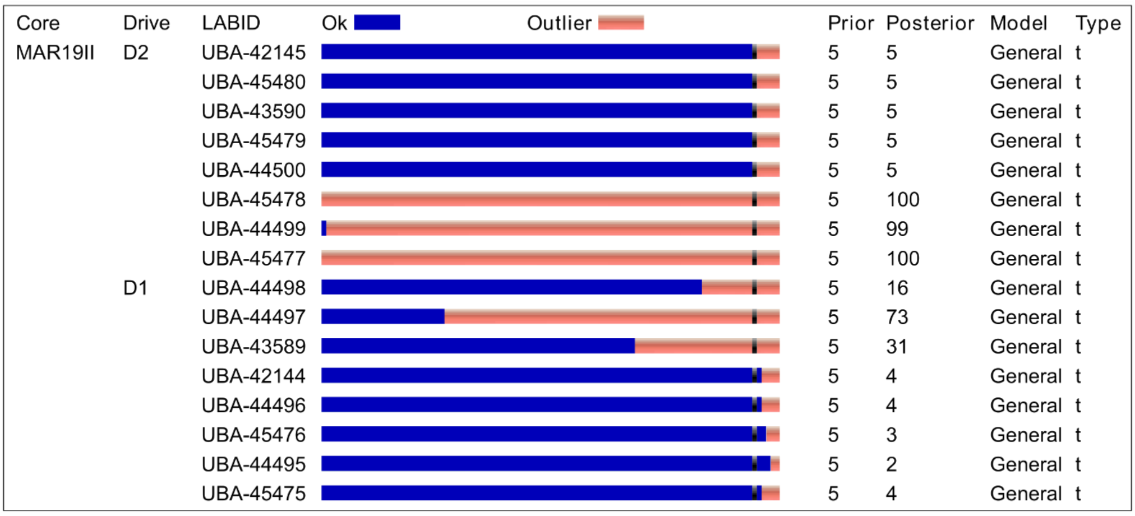

Core	Drive	LABID	Ok 🟦 Outlier 🟥	Prior	Posterior	Model	Type
MAR19II	D2	UBA-42145		5	5	General	t
		UBA-45480		5	5	General	t
		UBA-43590		5	5	General	t
		UBA-45479		5	5	General	t
		UBA-44500		5	5	General	t
		UBA-45478		5	100	General	t
		UBA-44499		5	99	General	t
		UBA-45477		5	100	General	t
	D1	UBA-44498		5	16	General	t
		UBA-44497		5	73	General	t
		UBA-43589		5	31	General	t
		UBA-42144		5	4	General	t
		UBA-44496		5	4	General	t
		UBA-45476		5	3	General	t
		UBA-44495		5	2	General	t
		UBA-45475		5	4	General	t

Appendix E: Coefficient correlation outputs between all identifiable fungi spores recorded from the sediments of Monquentiva.

Correlations are calculated using Pearson correlation coefficients using the concentration of fungi spore counts per cubic centimetre (cm^3), at both the 0.01 (**) and 0.05 (*) level of significance.

		Sporormiella	*A.imitans*	*Cercophora*	*Coniochaeta*	*Delitschia*	*Podospora*	*Sordaria*-type	*Trichodelitschia*	*Achaetomium*	*Chaetomium*	*Endophragmiella*	*Gelasinospora*	OU-5	OU-18 type	OU-100 type	OU108	*Preussia*-type	UAB1	UAB2	UAB7	UAB15	UAB30A	UAB32	UAB40	UAB48	UAB49	UAB50
Sporormiella	Pearson Correlation	1	.644**	.312*	.672**	.691**	.468**	.633**	.364**	.596**	-0.163	.278*	.507**	.624**	.351*	.770**	.549**	-0.246	-0.119	.325*	0.093	0.021	-0.105	0.002	0.171	0.249	0.018	.412**
	Sig. (2-tailed)		0.000	0.024	0.000	0.000	0.000	0.000	0.008	0.000	0.249	0.046	0.000	0.000	0.011	0.000	0.000	0.078	0.402	0.019	0.513	0.883	0.460	0.989	0.226	0.075	0.902	0.002
	N	52	52	52	52	52	52	52	52	52	52	52	52	52	52	52	52	52	52	52	52	52	52	52	52	52	52	52
A.imitans	Pearson Correlation	.644**	1	0.225	.714**	.722**	0.176	.574**	.749**	.334*	-0.020	0.069	0.152	.290*	.362**	.562**	.453**	-0.180	-0.090	.327*	0.195	-0.083	0.020	0.035	0.168	0.251	0.174	0.181
	Sig. (2-tailed)	0.000		0.108	0.000	0.000	0.213	0.000	0.000	0.016	0.888	0.627	0.282	0.037	0.008	0.000	0.001	0.201	0.528	0.018	0.165	0.560	0.887	0.804	0.234	0.073	0.216	0.200
	N	52	52	52	52	52	52	52	52	52	52	52	52	52	52	52	52	52	52	52	52	52	52	52	52	52	52	52
Cercophora	Pearson Correlation	.312*	0.225	1	.530**	0.069	.485**	.562**	-0.067	.598**	-0.059	.659**	0.094	.544**	.523**	.527**	.781**	-0.095	-0.043	.525**	0.234	-0.028	-0.093	-0.049	.480**	.536**	-0.064	-0.086
	Sig. (2-tailed)	0.024	0.108		0.000	0.626	0.000	0.000	0.637	0.000	0.680	0.000	0.510	0.000	0.000	0.000	0.000	0.504	0.763	0.000	0.095	0.844	0.510	0.730	0.000	0.000	0.654	0.546
	N	52	52	52	52	52	52	52	52	52	52	52	52	52	52	52	52	52	52	52	52	52	52	52	52	52	52	52
Coniochaeta	Pearson Correlation	.672**	.714**	.530**	1	.435**	.462**	.797**	.402**	.673**	-0.044	.363**	.364**	.648**	.529**	.829**	.733**	-0.105	0.076	.459**	.410**	0.027	-0.103	0.167	.325*	.481**	0.121	0.216
	Sig. (2-tailed)	0.000	0.000	0.000		0.001	0.001	0.000	0.003	0.000	0.758	0.008	0.008	0.000	0.000	0.000	0.000	0.460	0.594	0.001	0.003	0.852	0.466	0.237	0.019	0.000	0.392	0.124
	N	52	52	52	52	52	52	52	52	52	52	52	52	52	52	52	52	52	52	52	52	52	52	52	52	52	52	52
Delitschia	Pearson Correlation	.691**	.722**	0.069	.435**	1	0.138	.392**	.605**	0.246	-0.098	0.236	.374**	0.269	0.045	.423**	0.236	-0.114	0.007	0.032	0.061	-0.061	0.033	-0.049	0.148	-0.101	0.127	0.251
	Sig. (2-tailed)	0.000	0.000	0.626	0.001		0.330	0.004	0.000	0.079	0.490	0.092	0.006	0.054	0.750	0.002	0.092	0.421	0.960	0.823	0.666	0.667	0.818	0.728	0.297	0.475	0.370	0.072

N 52 52 52 52 52 52 52 52 52 52 52
52 52 52 52 52 52 52 52 52 52 52 52
52 52 52 52

Podospora Pearson Correlation .468** 0.176 .485** .462** 0.138 1 .586** -
0.133 .716** -0.117 .600** .281* .706** .403** .593** .644** -0.189 -0.085 0.175 -
0.003 0.208 -0.186 0.133 .485** .276* -0.127 0.077

Sig. (2-tailed) 0.000 0.213 0.000 0.001 0.330 0.000 0.347 0.000
0.411 0.000 0.044 0.000 0.003 0.000 0.000 0.181 0.548 0.214 0.982
0.139 0.186 0.347 0.000 0.047 0.370 0.585

N 52 52 52 52 52 52 52 52 52 52 52
52 52 52 52 52 52 52 52 52 52 52 52
52 52 52 52

Sordaria-type Pearson Correlation .633** .574** .562** .797** .392** .586** 1
0.206 .809** -0.076 .460** .337* .685** .773** .853** .840** -0.173 -0.074
.544** .347* -0.023 -0.028 0.167 .670** .446** 0.047 0.166

Sig. (2-tailed) 0.000 0.000 0.000 0.000 0.004 0.000 0.144 0.000
0.591 0.001 0.015 0.000 0.000 0.000 0.000 0.221 0.602 0.000 0.012
0.870 0.843 0.237 0.000 0.001 0.743 0.239

N 52 52 52 52 52 52 52 52 52 52 52
52 52 52 52 52 52 52 52 52 52 52 52
52 52 52 52

Trichodelitschia Pearson Correlation .364** .749** -0.067 .402** .605** -0.133 0.206 1
-0.095 -0.098 -0.060 0.215 -0.086 -0.077 0.248 -0.037 -0.103 -0.072 -0.087
0.077 -0.047 -0.061 -0.082 -0.067 -0.091 0.090 0.010

Sig. (2-tailed) 0.008 0.000 0.637 0.003 0.000 0.347 0.144 0.504
0.490 0.675 0.127 0.543 0.588 0.077 0.794 0.465 0.614 0.542 0.586
0.742 0.669 0.564 0.637 0.520 0.524 0.946

N 52 52 52 52 52 52 52 52 52 52 52
52 52 52 52 52 52 52 52 52 52 52 52
52 52 52 52

Achaetomium Pearson Correlation .596** .334* .598** .673** 0.246 .716** .809** -
0.095 1 -0.083 .605** .324* .958** .705** .776** .919** -0.134 -0.061 .411**
0.136 -0.040 -0.132 0.011 .598** .369** -0.090 0.202

Sig. (2-tailed) 0.000 0.016 0.000 0.000 0.079 0.000 0.000 0.504
0.559 0.000 0.019 0.000 0.000 0.000 0.000 0.343 0.670 0.002 0.335
0.780 0.350 0.940 0.000 0.007 0.525 0.151

N 52 52 52 52 52 52 52 52 52 52 52
52 52 52 52 52 52 52 52 52 52 52 52
52 52 52 52

Chaetomium Pearson Correlation -0.163 -0.020 -0.059 -0.044 -0.098 -0.117 -0.076 -
0.098 -0.083 1 -0.052 -0.117 -0.075 -0.067 -0.113 -0.048 0.222 0.249 -0.076
.536** -0.041 .591** 0.058 -0.059 -0.020 .384** .593**

Sig. (2-tailed) 0.249 0.888 0.680 0.758 0.490 0.411 0.591 0.490 0.559
0.714 0.408 0.595 0.636 0.427 0.734 0.114 0.076 0.594 0.000 0.773
0.000 0.683 0.680 0.890 0.005 0.000

N 52 52 52 52 52 52 52 52 52 52 52
52 52 52 52 52 52 52 52 52 52 52 52
52 52 52 52

Endophragmiella Pearson Correlation .278* 0.069 .659** .363** 0.236 .600** .460** -
0.060 .605** -0.052 1 .315* .617** 0.137 .431** .595** -0.084 -0.038 -0.046
0.058 -0.025 -0.083 -0.044 .659** -0.049 -0.057 0.076

Sig. (2-tailed) 0.046 0.627 0.000 0.008 0.092 0.000 0.001 0.675 0.000
0.714 0.023 0.000 0.335 0.001 0.000 0.552 0.789 0.745 0.683
0.861 0.557 0.759 0.000 0.732 0.690 0.591

N 52 52 52 52 52 52 52 52 52 52 52
52 52 52 52 52 52 52 52 52 52 52 52
52 52 52 52

Gelasinospora Pearson Correlation .507** 0.152 0.094 .364** .374** .281* .337*
0.215 .324* -0.117 .315* 1 .394** -0.016 .351* 0.205 -0.066 -0.086
0.025 0.168 0.187 -0.044 -0.056 0.094 -0.109 -0.017 0.172

Sig. (2-tailed) 0.000 0.282 0.510 0.008 0.006 0.044 0.015 0.127 0.019
0.408 0.023 0.004 0.910 0.011 0.145 0.640 0.546 0.862 0.234
0.184 0.757 0.695 0.510 0.440 0.905 0.224

N 52 52 52 52 52 52 52 52 52 52 52
52 52 52 52 52 52 52 52 52 52 52 52
52 52 52 52

OU-5 Pearson Correlation .624** .290* .544** .648** 0.269 .706** .685** -0.086
.958** -0.075 .617** .394** 1 .495** .761** .820** -0.122 -0.055 .319*
0.092 -0.036 -0.120 -0.027 .395** .302* -0.082 .282*

Sig. (2-tailed) 0.000 0.037 0.000 0.000 0.054 0.000 0.000 0.543 0.000
0.595 0.000 0.004 0.000 0.000 0.000 0.389 0.698 0.021 0.517
0.799 0.395 0.851 0.004 0.030 0.563 0.043

N 52 52 52 52 52 52 52 52 52 52 52
52 52 52 52 52 52 52 52 52 52 52 52
52 52 52 52

OU-18 type Pearson Correlation .351* .362** .523** .529** 0.045 .403** .773** -
0.077 .705** -0.067 0.137 -0.016 .495** 1 .552** .808** -0.109 -0.049 .656**
0.226 -0.032 -0.107 0.083 .637** .584** -0.073 -0.061

Sig. (2-tailed) 0.011 0.008 0.000 0.000 0.750 0.003 0.000 0.588 0.000
0.636 0.335 0.910 0.000 0.000 0.000 0.442 0.729 0.000 0.107
0.821 0.448 0.558 0.000 0.000 0.606 0.668

N 52 52 52 52 52 52 52 52 52 52 52
52 52 52 52 52 52 52 52 52 52 52 52
52 52 52 52

OU-100 type Pearson Correlation .770** .562** .527** .829** .423** .593** .853**
0.248 .776** -0.113 .431** .351* .761** .552** 1 .737** -0.200 -0.094
.476** .299* -0.028 -0.102 -0.023 .373** .348* 0.086 .345*

Sig. (2-tailed) 0.000 0.000 0.000 0.000 0.002 0.000 0.000 0.077 0.000
0.427 0.001 0.011 0.000 0.000 0.000 0.156 0.508 0.000 0.031
0.845 0.472 0.870 0.007 0.011 0.543 0.012

N 52 52 52 52 52 52 52 52 52 52 52
52 52 52 52 52 52 52 52 52 52 52 52
52 52 52 52

OU108 Pearson Correlation .549** .453** .781** .733** 0.236 .644** .840** -0.037
.919** -0.048 .595** 0.205 .820** .808** .737** 1 -0.133 -0.048 .582**
0.254 -0.047 -0.095 0.070 .668** .525** -0.011 0.098

Sig. (2-tailed) 0.000 0.001 0.000 0.000 0.092 0.000 0.000 0.794 0.000
0.734 0.000 0.145 0.000 0.000 0.000 0.348 0.736 0.000 0.070
0.740 0.501 0.623 0.000 0.000 0.937 0.491

N 52 52 52 52 52 52 52 52 52 52 52
52 52 52 52 52 52 52 52 52 52 52 52
52 52 52 52

Preussia-type Pearson Correlation -0.246 -0.180 -0.095 -0.105 -0.114 -0.189 -0.173 -
0.103 -0.134 0.222 -0.084 -0.066 -0.122 -0.109 -0.200 -0.133 1 .320* -0.123
0.047 -0.066 .286* 0.005 -0.095 -0.073 0.215 0.000

Sig. (2-tailed) 0.078 0.201 0.504 0.460 0.421 0.181 0.221 0.465 0.343
0.114 0.552 0.640 0.389 0.442 0.156 0.348 0.021 0.387 0.740
0.640 0.040 0.974 0.504 0.606 0.126 1.000

N 52 52 52 52 52 52 52 52 52 52 52
52 52 52 52 52 52 52 52 52 52 52 52
52 52 52 52

UAB1 Pearson Correlation -0.119 -0.090 -0.043 0.076 0.007 -0.085 -0.074 -0.072 -
0.061 0.249 -0.038 -0.086 -0.055 -0.049 -0.094 -0.048 .320* 1 -0.055 0.178 -
0.030 0.206 0.165 -0.043 0.043 0.168 -0.018

Sig. (2-tailed) 0.402 0.528 0.763 0.594 0.960 0.548 0.602 0.614 0.670
0.076 0.789 0.546 0.698 0.729 0.508 0.736 0.021 0.697 0.207
0.833 0.143 0.241 0.763 0.763 0.234 0.898

N 52 52 52 52 52 52 52 52 52 52 52
52 52 52 52 52 52 52 52 52 52 52 52
52 52 52 52

UAB2 Pearson Correlation .325* .327* .525** .459** 0.032 0.175 .544** -0.087
.411** -0.076 -0.046 0.025 .319* .656** .476** .582** -0.123 -0.055 1
.407** -0.036 0.091 0.078 0.141 .629** -0.082 -0.111

Sig. (2-tailed) 0.019 0.018 0.000 0.001 0.823 0.214 0.000 0.542 0.002
0.594 0.745 0.862 0.021 0.000 0.000 0.000 0.387 0.697 0.003
0.799 0.523 0.583 0.320 0.000 0.561 0.434

N 52 52 52 52 52 52 52 52 52 52 52
52 52 52 52 52 52 52 52 52 52 52 52
52 52 52 52

UAB7 Pearson Correlation 0.093 0.195 0.234 .410** 0.061 -0.003 .347* 0.077
0.136 .536** 0.058 0.168 0.092 0.226 .299* 0.254 0.047 0.178 .407** 1
-0.073 .346* .314* 0.121 .294* .289* .297*

Sig. (2-tailed) 0.513 0.165 0.095 0.003 0.666 0.982 0.012 0.586 0.335
0.000 0.683 0.234 0.517 0.107 0.031 0.070 0.740 0.207 0.003
0.608 0.012 0.023 0.391 0.035 0.038 0.033

N 52 52 52 52 52 52 52 52 52 52 52
52 52 52 52 52 52 52 52 52 52 52 52
52 52 52 52

UAB15 Pearson Correlation 0.021 -0.083 -0.028 0.027 -0.061 0.208 -0.023 -0.047 -
0.040 -0.041 -0.025 0.187 -0.036 -0.032 -0.028 -0.047 -0.066 -0.030 -0.036 -0.073 1
-0.065 -0.034 -0.028 -0.038 -0.045 -0.060

Sig. (2-tailed) 0.883 0.560 0.844 0.852 0.667 0.139 0.870 0.742 0.780
0.773 0.861 0.184 0.799 0.821 0.845 0.740 0.640 0.833 0.799 0.608
0.645 0.809 0.844 0.788 0.754 0.673

	N	52	52	52	52	52	52	52	52	52	52	52
	52	52	52	52	52	52	52	52	52	52	52	52
	52	52	52	52								
UAB30A	Pearson Correlation			-0.105	0.020	-0.093	-0.103	0.033	-0.186	-0.028	-0.061	-
0.132	.591**	-0.083	-0.044	-0.120	-0.107	-0.102	-0.095	.286*	0.206	0.091	.346*	-
0.065	1	-0.044	-0.093	-0.127	.337*	.318*						
	Sig. (2-tailed)		0.460	0.887	0.510	0.466	0.818	0.186	0.843	0.669	0.350	
	0.000	0.557	0.757	0.395	0.448	0.472	0.501	0.040	0.143	0.523	0.012	
	0.645		0.754	0.510	0.368	0.015	0.022					
	N	52	52	52	52	52	52	52	52	52	52	52
	52	52	52	52	52	52	52	52	52	52	52	52
	52	52	52	52								
UAB32	Pearson Correlation			0.002	0.035	-0.049	0.167	-0.049	0.133	0.167	-0.082	
	0.011	0.058	-0.044	-0.056	-0.027	0.083	-0.023	0.070	0.005	0.165	0.078	
	.314*	-0.034	-0.044	1	0.078	.541**	.354**	0.063				
	Sig. (2-tailed)		0.989	0.804	0.730	0.237	0.728	0.347	0.237	0.564	0.940	
	0.683	0.759	0.695	0.851	0.558	0.870	0.623	0.974	0.241	0.583	0.023	
	0.809	0.754		0.581	0.000	0.010	0.658					
	N	52	52	52	52	52	52	52	52	52	52	52
	52	52	52	52	52	52	52	52	52	52	52	52
	52	52	52	52								
UAB40	Pearson Correlation			0.171	0.168	.480**	.325*	0.148	.485**	.670**	-0.067	
	.598**	-0.059	.659**	0.094	.395**	.637**	.373**	.668**	-0.095	-0.043	0.141	
	0.121	-0.028	-0.093	0.078	1	0.064	-0.064	-0.086				
	Sig. (2-tailed)		0.226	0.234	0.000	0.019	0.297	0.000	0.000	0.637	0.000	
	0.680	0.000	0.510	0.004	0.000	0.007	0.000	0.504	0.763	0.320	0.391	
	0.844	0.510	0.581		0.654	0.654	0.546					
	N	52	52	52	52	52	52	52	52	52	52	52
	52	52	52	52	52	52	52	52	52	52	52	52
	52	52	52	52								
UAB48	Pearson Correlation			0.249	0.251	.536**	.481**	-0.101	.276*	.446**	-0.091	
	.369**	-0.020	-0.049	-0.109	.302*	.584**	.348*	.525**	-0.073	0.043	.629**	
	.294*	-0.038	-0.127	.541**	0.064	1	0.114	-0.039				
	Sig. (2-tailed)		0.075	0.073	0.000	0.000	0.475	0.047	0.001	0.520	0.007	
	0.890	0.732	0.440	0.030	0.000	0.011	0.000	0.606	0.763	0.000	0.035	
	0.788	0.368	0.000	0.654		0.422	0.784					
	N	52	52	52	52	52	52	52	52	52	52	52
	52	52	52	52	52	52	52	52	52	52	52	52
	52	52	52	52								
UAB49	Pearson Correlation			0.018	0.174	-0.064	0.121	0.127	-0.127	0.047	0.090	-
0.090	.384**	-0.057	-0.017	-0.082	-0.073	0.086	-0.011	0.215	0.168	-0.082	.289*	-
0.045	.337*	.354**	-0.064	0.114	1	.590**						
	Sig. (2-tailed)		0.902	0.216	0.654	0.392	0.370	0.370	0.743	0.524	0.525	
	0.005	0.690	0.905	0.563	0.606	0.543	0.937	0.126	0.234	0.561	0.038	
	0.754	0.015	0.010	0.654	0.422		0.000					
	N	52	52	52	52	52	52	52	52	52	52	52
	52	52	52	52	52	52	52	52	52	52	52	52
	52	52	52	52								

UAB50 Pearson Correlation .412** 0.181 -0.086 0.216 0.251 0.077 0.166 0.010
0.202 .593** 0.076 0.172 .282* -0.061 .345* 0.098 0.000 -0.018 -0.111
.297* -0.060 .318* 0.063 -0.086 -0.039 .590** 1

Sig. (2-tailed) 0.002 0.200 0.546 0.124 0.072 0.585 0.239 0.946 0.151
0.000 0.591 0.224 0.043 0.668 0.012 0.491 1.000 0.898 0.434 0.033
0.673 0.022 0.658 0.546 0.784 0.000

N 52 52 52 52 52 52 52 52 52 52 52
52 52 52 52 52 52 52 52 52 52 52 52
52 52 52 52

**. Correlation is significant at the 0.01 level (2-tailed) *. Correlation is significant at the 0.05 level (2-tailed).

REFERENCES

3d_Moiler., 2014. B*lack Alder tree (Alnus glutinosa)*, TURBOSQUID by shutterstock, viewed 10 January 2022, <https://www.turbosquid.com/3d-models/black-alder tree alnus-3d-model/830296>.

Abràmoff, M.D., Magalhães, P.J. and Ram, S.J., 2004. Image processing with ImageJ. Biophotonics international, 11(7): 36-42.

Alfonso- Rojas, A., Herrera-Gutierrez, L.M., Suárez, C., M., Ciancio, M.R., Pelegrin, J.S. and Cadena, E-A., 2021. 'Late Pleistocene Biota from Pubenza, Colombia; Turtles, Mammals, Birds, Invertebrates and Plant Remains'. *Journal of Quaternary Science,* 36(3): 450–66.

Amador, M. and Millner, N., 2019. *Páramo de Monquentiva: Introducing the field sites from the SocioCultural Component,* accessed 23 March 2022, <https://blogs.exeter.ac.uk/bioresilience/blog/2019/09/27/introducing-the-field sites from-the sociocultural-perspective-1-monquentiva-cundimarca>.

Archila, S., Groot, A.M., Ospina, J.P., Mejía, M. and Zorro, C., 2021. Dwelling the hill: Traces of increasing sedentism in hunter-gatherers societies at Checua site, Colombia (9500-5052 cal BP). *Quaternary International*, 578: 102-119.

Arif, F., 2020. *According to a recent study, evidence from the hunter gatherer society suggest that the gender disparities are not so natural*, accessed 02 July 2022, <https://pk.mashable.com/science/5825/according-to-a-recent-study-evidence from-the-hunter-gatherer-society-suggest-that-the-gender-dispar>.

Avella, A.M, Torres, S.R., Gómez, W.A. and Pardo, M.P., 2014. The paramos and high Andean forests of the Monquentiva swamp or Martos swamp (Guatavita, Cundinamarca, Colombia): ecological characterization and conservation status, *Biota Colombiana*, 15(1): 3-39.

Baena, J., Carrión, E. and Blasco, C., 2004. *Rock art findings in the Chiribiquete mountain range*, Colombia. Archaeological mission 1992, Rupestreweb.

Barnosky, A.D. and Lindsey, E.L., 2010. Timing of Quaternary megafaunal extinction in South America in relation to human arrival and climate change, *Quaternary International*, 217: 10-29.

Barnosky, A.D., Koch, P.L., Feranec, R.S., Wing, S.L. and Shabel, A.B., 2004. Assessing the causes of Late Pleistocene Extinctions on the Continents, *Science*, 306(5693): 70-75.

Benedek., 2015. *Traditional Kogi Hut in Colombia, South America*. Benedek, Canada, viewed 14 January 2022, <https://www.istockphoto.com/photo/traditional-kogi hut in-sierra-nevada-de santa-marta-colombia-gm501625816-81436861>.

Becerra, M., 1995. *Études morphologiques et traceologiques des micro pointes de quartz de 'Duitama-Tocogua'*, Haut Plateau de Boyacá en Colombia. Université de Paris-I, Panthéon Sorbonne. Crap, Paris.

Bernal, R., Gradstein, S.R and Celis, M. eds., 2019. *Catálogo de Plantas Y Líquenes de Colombia*, Institute of Natural Sciences, Universidad Nacional de Colombia, Bogotá. [online], viewed 17 May 2021, Available at <http://catalogoplantasdecolombia.unal.edu.co/en/>.

Bischler, H., and Pinto, P. (1959). *Cave paintings and engravings in the Serranía de la Macarena*. In Lamp Magazine, International Petroleum Company, Bogota, 6 (31): 1415.

Blaauw, M. and Christen, J.A., 2013. Bacon Manual e v2.3.9.1, *School of Natural and Built Environment*: 1-13.

Bogotá-A, R.G., Groot, M.H.M., Hooghiemstra, H., Lourens, L.J., Van der Linden, M. and Berrio, J.C., 2011. Rapid climate change from north Andean Lake Fúquene pollen records driven by obliquity: implications for a basin-wide Biostratigraphic zonation for the last 284 ka. *Quaternary Science Reviews*, 30(23-24): 3321 3337.

Borrero, L.A., 2009. The Elusive Evidence: *The Archaeological Record of the South American Extinct Megafauna, in American Megafaunal Extinctions at the End of the Pleistocene*, Dordrecht, Springer, 145-168.

Borrero, L.A., Zarate, M., Miotti, L., Massone, M., 1998. The Pleistocene-Holocene transition and human occupations in the southern cone of South America. *Quaternary International,* 49–50: 191–199.

Bufalo, F.S., Galetti, M. and Culot, L., 2016. Seed dispersal by primates and implications for the conservation of a biodiversity hotspot, the Atlantic forest of South America. *International Journal of Primatology*, *37*: 333-349.

Burney, D.A., Robinson, G.S. and Burney, L.P., 2003. Sporormiella and the late Holocene extinctions in Madagascar. *Proceedings of the National Academy of Sciences*, 100(19): 10800-10805.

Bush, M.B., Alfonso- Reynolds, A.M., Urrego, D.H., Valencia, B.G., Correa- Metrio, Y.A., Zimmermann, M. and Silman, M.R., 2015. Fire and climate: contrasting pressures on tropical Andean timberline species. *Journal of Biogeography*, 42(5): 938-950.

Bush, M.B. and Weng, M.B., 2006. Introducing a new (freeware) tool for palynology. *Journal of Biogeography*, 34(3): 377-380.

CAR., 2000. *Regional Autonomous Corporation of Cundinamarca, Guatavita Cundinamarca, Land Management Scheme*, Bogota, Colombia: 1-101.

CAR., 2007. *Elaboración del Diagnostico, Prospectiva y Formulación Cuenca Hidrográfica del Río Gacheta Subcuenca Río Monquentiva*. Bogotá: CAR.

Carreño T.G. 2017. *An Illustration of Pleistocene megafaunal species,* in Hace tiempo. Un viaje paleontológico ilustrado por Colombia. Instituto Alexander von Humboldte Instituto Smithsonian de Investigaciones Tropicales. Bogotá, Colombia, [viewed 27 May 2022]: 66-67.

Chepstow-Lusty, A.J., Frogley, M.R. and Baker, A.S., 2019. Comparison of *Sporormiella* dung fungal spores and oribatid mites as indicators of large herbivore presence: evidence from the Cuzco region of Peru. *Journal of Archaeological Science*, 102: 61-70.

Clark, J.S. and Patterson, W.A., 1997. Background and local charcoal in sediments: scales of fire in the paleorecord, In Clark, J.S., Cachier, H., Goldammer, J.G and Stocks, B. ed(s) *Sediment records of biomass burning and global change*, *Springer*, Berlin: 23-48.

Clark, J.S., Royall, D.P. and Chumbley, C. 1996. 'The Role of Fire During Climate Change in an Eastern Deciduous Forest at Devil's Bathtub, New York'. *Ecology* 77(7): 2148-66.

Colinvaux, P.A., De Oliveira, P.E. and M.B. Bush., (2000) 'Amazonian and Neotropical Plant Communities on Glacial Time-Scales: The Failure of the Aridity and Refuge Hypotheses'. *Quaternary Science Reviews* (19): 141–169.

Colinvaux, P.A., De Oliveira, P.E., Moreno, J.E., 1999. *Amazon Pollen Manual and Atlas. Harwood Academic Press*, New York.

Coltorti, M., Ficcarelli, G., Jahren, H., Espinosa, M.M., Rook, L. and Torre, D., 1998. The last occurrence of Pleistocene megafauna in the Ecuadorian Andes. *Journal of South American Earth Sciences*, 11(6): 581-586.

Conroy, K.J., Baker, A.G., Jones, V.J., van Hardenbroek, M., Hopla, E.J., Collier, R., Lister, A.M. and Edwards, M.E., 2020. Tracking late-Quaternary extinctions in interior Alaska using megaherbivore bone remains and dung fungal spores, *Quaternary Research*, 97: 99-110.

Cooke, R., 1998. 'HUMAN SETTLEMENT OF CENTRAL AMERICA AND NORTHERNMOST SOUTH AMERICA (14,000–8000BP)', *Quaternary International,* 49–50: 177–90.

Cooper, A., Turney, C., Hughen, K. A., Brook, B.W., McDonald, H. G. and Bradshaw, C.J.A., 2015. Abrupt warming events drove Late Pleistocene Holarctic megafaunal turnover, *Science,* 349(6248): 602-606.

Correal, G., Piñeros, F. and Van Der Hammen, T., 1990. Guayabero I: un sitio precerámico de la localidad Angostura II, San José del Guaviare. *Caldasia*: 245-254.

Correal-Urrego, G., 1981. *Evidencias culturales y megafauna Pleistocénica en Colombia*. Fundación de Investigaciones Arqueológicas Nacionales, Banco de la República, Bogotá

Correal-Urrego, G., 1993. New Pleistocene cultural evidences and megafauna in Colombia, *Archeology Bulletin,* 8(1): 3-12. doi.org/10.1007/978-1-4020-879368.

Correal-Urrego, G., Olano, J.G., Calderón, K.J. and Cardozo, D.C.V., 2005. Archaeological evidence and extinct megafauna in a salt flat from the Upper Tardiaglacial. *Archeology Bulletin,* 20: 3-58.

Cronquist, A., 1988. *The evolution and Classification of Flowering Plants*. The New York Botanical Garden, Bronx, New York.

Crystal-Arens, N., 2001. Variation in performance of the tree fern Cyathea caracasana (Cyatheaceae) across a successional mosaic in the Andean cloud forest, *American Journal of Botany,* 88(3): 545-551.

Cugny, C., Mazier, F. and Galop, D., 2010. ‘Modern and Fossil Non-Pollen Palynomorphs from the Basque Mountains (Western Pyrenees, France): the Use of Coprophilous Fungi to Reconstruct Pastoral Activity’. *Vegetation History and Archaeobotany* 19: 391–408.

Dantas, V. L. and Pausas, J.G., 2022. The legacy of the extinct Neotropical megafauna on plants and biomes, *Nature communications*, 13(129): 1–13.

Davis, O.K., Agenbroad, L., Martin, P.S. and Mead, J.I., 1984. The Pleistocene dung blanket of Bechan Cave, Utah. *Special Publications of the Carnegie Museum of Natural History,* 8: 267–282.

Davis, O.K., 1987. Spores of the dung fungus *Sporormiella*: increased abundance in historic sediments and before Pleistocene megafaunal extinction, *Quaternary Research*, 28(2): 290-294.

Davis, O.K. and Shafer, D.S., 2006. Sporormiella fungal spores, a palynological means of detecting herbivore density, *Paleogeography, Palaeoclimatology, Palaeoecology*, 237(1): 40-50.

Dickinson, C.H. and Underhay, V.H.S., 1977. Growth of fungi in cattle dung. *Transactions of the British Mycological Society*, 69(3): 473-477.

Dix, N.J. and Webster, J., 1995. *Fungal ecology,* London, Chapman and Hall.

Elias, S.A. and Schreve, D., 2007. Late Pleistocene Megafaunal Extinctions, *Elsevier*: 3202-3217.

Escribano-Avila, G., Lara-Romero, C., Heleno, R. and Traveset, A., 2018. Tropical seed dispersal networks: emerging patterns, biases, and keystone species traits. *Ecological networks in the tropics: an integrative overview of species interactions from some of the most species-rich habitats on earth*: 93-110.

Espinoza, I.G., Franco-Gaviria, F., Castañeda, I., Robinson, C., Room, A., Berrío, J.C., Armenteras, D. and Urrego, D.H. (2022) Holocene fires and ecological novelty in the high Colombian Coredillera Oriental. *Frontiers in Ecology and Evolution*, 10: 1-16.

Etienne, D., Wilhelm, B., Sabatier, P., Reyss, J.L. and Arnaud, F., 2013. Influence of sample location and livestock numbers on Sporormiella concentrations and accumulation rates in surface sediments of Lake Allos, French Alps. *Journal of Paleolimnology*, 49(2):117-127.

Etienne, D. and Jouffroy-Bapicot, I., 2014. ‘Optimal Counting Limit for Fungal Spore Abundance Estimation Using *Sporormiella* as a Case Study’. *Vegetation History and Archaeobotany* 23(6): 743–49.

Fægri, K., Kaland, P.E. and Krzywinski, K., 1989. *Textbook of pollen analysis*, John Wiley & Sons Ltd.

Ficcarelli, G., Azzaroli, A., Bertini, A., Coltorti, M., Mazza, P., Mezzabotta, C., Espinosa, M.M., Rook, L. and Torre, D., 1997. Hypothesis on the cause of extinction of the South American mastodonts. *Journal of South American Earth Sciences*, 10(1): 29-38.

Firestone, R.B., West, A., Kennett, J.P., Becker, L., Bunch, T.E., Revay, Z.S., Schultz, P.H., Belgya, T., Kennett, D.J., Erlandson, J.M. and Dickenson, O.J., 2007. Evidence for an extraterrestrial impact 12,900 years ago that contributed to the megafaunal extinctions and the Younger Dryas cooling. *Proceedings of the National Academy of Sciences*, 104(41): 16016-16021.

Galetti, M., Moleón, M., Jordano, P., Pires, M.M., Guimaraes Jr, P.R., Pape, T., Nichols, E., Hansen, D., Olesen, J.M., Munk, M. and de Mattos, J.S., 2018. Ecological and evolutionary legacy of megafauna extinctions. *Biological Reviews*, *93*(2): 845-862.

Garcia, M., 2022. *Cloud PNG*, 123PNGDownload, viewed 15 January 2022, <https://123pngdownload.com/cloud-png-images/>.

García-Rangel, S., 2012. Andean bear *Tremarctos ornatus* natural history and conservation, *Mammal review*, 42(2): 85-110.

Gentry, A.H., 1993. *A field guide to the families and genera of woody plants of northwest South America (Colombia, Ecuador, Peru), with supplementary notes on herbaceous taxa*. Conservation International, Washington, DC.

Gill, J.L., McLauchlan, K.K., Skibbe, A.M., Goring, S., Zirbel, C.R. and Williams, J.W., 2013. Linking abundances of the dung fungus *Sporormiella* to the density of bison: implications for assessing grazing by megaherbivores in palaeorecords. *Journal of Ecology*, 101(5): 1125-1136.

Gill, J.L., Williams, J.W., Jackson, S.T., Donnelly, J.P. and Schellinger, G.C., 2012. Climatic and megaherbivory controls on late-glacial vegetation dynamics: a new, high resolution, multi proxy record from Silver Lake, Ohio, *Quaternary Science Reviews*, 34: 66-80.

Gill, J.L., Williams, J.W., Jackson, S.T., Lininger, K.B. and Robinson, G.S., 2009. 'Pleistocene Megafaunal Collapse, Novel Plant Communities, and Enhanced Fire Regimes in North America', *Science,* 326(5): 1100-1103.

Gómez, A., Berrío, J.C., Hooghiemstra, H. Becerra, M. and Marchant, R., 2007. A Holocene pollen record of vegetation change and human impact from Pantano de Vargas, an intra-Andean basin of Duitama, Colombia, *Review of Palaeobotany and Palynology*, 145: 143-157.

Gomez, C.L. and Rubio, D., 2003. *The martos reservoir: historical, cultural and geographical study*. Academy of History of Cundinamarca and Secretary of the Environment of the department of Cundinamarca, 1-103.

Gordon, C.E., Rion E.L., Allin, P., Greve, M. and Svenning, J-S., 2021. 'Elephant rewilding indirectly affects the abundance of an arboreal but not generalist Savanna Lizard'. *Biodiversity and Conservation*, 30(5):1277-1291.

Grabandt, R.A.J., 1980. Pollen rain in relation to arboreal vegetation in the Colombian Cordillera Oriental, *Review of Palaeobotany and Palynology,* 29: 65-147.

Guarro, J., Gené, J., Stchigel, A.M. and Figueras, M.J., 2012. *Atlas of soil ascomycetes*, CBS-KNAW Fungal Biodiversity Centre, Utrecht.

Hagemans, K., Tóth, C.D., Ormaza, M., Gosling, W.D., Urrego, D.H., León-Yánez, S., Wagner-Cremer, F. and Donders, T.H., 2019. Modern pollen-vegetation relationships along a steep temperature gradient in the Tropical Andes of Ecuador. *Quaternary Research*, 92(1): 1-13.

Halbwachs, H. and Bässler, C., 2020. No bull: Dung-dwelling mushrooms show reproductive trait syndromes different from their non-coprophilous allies. *Mycological Progress*, 19(8): 817-824.

Halsall, K.M., Ellingsen, V.M., Asplund, J., Bradshaw, R.H.W. and Ohlson, M., 2018. Fossil charcoal quantification using manual and image analysis approaches, *The Holocene*, 28(8): 1345-1353.

Higuera, P., 2009. *CharAnalysis 0.9: Diagnostic and analytical tools for sediment charcoal analysis*. User's Guide, Montana State University, Missoula, USA.

Higuera, P.E., Brubaker, L.B., Anderson, P.M., Hu, F.S. and Brown, T.A., 2009. Vegetation mediated the impacts of postglacial climatic change on fire regimes in the south central Brooks Range, Alaska. *Ecological Monographs*, 79: 201 219.

Hooghiemstra, H. and Flantua, S.G.A., 2019. Colombia in the Quaternary: An overview of environmental and climatic change. In: Gómez, J. and Pinilla–Pachon, A.O. (eds.), *The Geology of Colombia*, Servicio Geológico Colombiano, Publicaciones Geológicas Especiales, Bogotá, 4(38): 43 95.

Hooghiemstra, H. and van der Hammen, T., 1993. Late Quaternary vegetation history and paleoecology of Laguna Pedro Palo (subandean forest belt, Eastern Cordillera, Colombia), *Review of Palaeobotany and Palynology*, 77: 235-262.

Hooghiemstra, H., 1984. *Vegetational and Climatic History of the High Plain of Bogotá, Colombia: A Continuous Record of the Last 3.5 Million Years*, Cramer, Germany.

IBM Corp., 2020. *IBM SPSS Statistics for Windows*, Version 26.0, Armonk, New York, IBM Corp.

Inkscape Project., 2022. Inkscape v.1.1.2, Inkscape's Contributors (vendor), annual updating.

Johnson, C.N., 2009. Ecological consequence of Late Quaternary extinctions of megafauna, *Proceedings of The Royal Society*, 276: 2509-2519.

Johnson, C.N., Rule, S. Haberle, S.G., Turney, C.S.M., Kershaw, A.P. and Brook, B.W., 2015. Using dung fungi to interpret decline and extinction of megaherbivores: problems and solutions, *Quaternary science Reviews,* 110: 107-113.

Juggins, S., 2007. *C2: Software for ecological and palaeoecological data analysis and visualisation (User guide version 1.5)*, Newcastle, Newcastle University: 1-73.

Jull, A.J.T., Iturralde-Vinent, M., O'malley, J.M., MacPhee, R.D.E., McDonald, H.G., Martin, P.S., Moody, J. and Rincón, A., 2004. Radiocarbon dating of extinct fauna in the Americas recovered from tar pits. *Nuclear Instruments and Methods in Physics Research Section B: Beam Interactions with Materials and Atoms*, 223: 668-671.

Kammer, A., Piraquive, A., Gómez, C., Mora, A., Velásquez, A., Gómez, J. and Mateus Zabala, D., 2020. Structural styles of the Eastern Cordillera of Colombia. *The geology of Colombia*, 3: 37-41.

Kershaw, A.P., 1997. A modification of the Troels-Smith system of sediment description and portrayal, *Quaternary Australasia*, 15(2): 63-68.

Krug, J.C., Benny, G.L. and Keller, H.W., 2004. Coprophilous fungi, in: Mueller, G.M., Bills, G.F. and Foster, M.S. ed(s). *Biodiversity of Fungi, Inventory and Monitoring Methods*, Elsevier, Burlington: 467–499.

Kuthubutheen, A.J. and Webster, J., 1986. Water availability and the coprophilous fungus succession. *Transactions of the British Mycological Society*, 86(1): 63 -76.

Langbaek C. H., 2001. *Arqueologia regional en el Valle de Leiva: procesos de ocupacion humana en una region de los Andes orientales de Colombia*. Colombiano de Antropologia e Historia. Bogota. Colombia.

Langebaek, C. H., 1985. Cuando los Muiscas diversificaron la agricultura y crearon el intercambio, *Boletín Cultural Y Bibliográfico*, 22(3): 3-10.

Last, W.M. and Smol, J.P. eds., 2002. *Tracking environmental change using lake sediments: volume 1: basin analysis, coring and chronological techniques* (Vol.1), Springer, Science & Business Media.

Lee, C.M., van Geel, B. and Gosling, W.D., 2022. On the Use of Spores of Coprophilous Fungi Preserved in Sediments to Indicate Past Herbivore Presence. *Quaternary*, 5(30): 1-25.

Lima-Ribeiro, M.S. and Diniz-Filho, J.A.F., 2013. American megafaunal extinctions and human arrival: Improved evaluation using a meta-analytical approach, *Quaternary International*, 38-52.

Loughlin, N. J.D., Gosling, W.D. and Montoya, E., 2018. 'Identifying Environmental Drivers of Fungal Non-Pollen Palynomorphs in the Montane Forest of the Eastern Andean Flank, Ecuador'. *Quaternary Research* 89(1): 119-133.

Lüttge, U. ed., 2007. *Clusia: a woody neotropical genus of remarkable plasticity and diversity*. Springer, New York.

MacPhee, R.D. and Sues, H.D. eds., 1999. *Extinctions in near time* (Vol. 2). Springer Science & Business Media.

Maher Jr, L.J., 1981. Statistics for microfossil concentration measurements employing samples spiked with marker grains, *Review of Palaeobotany and Palynology,* 32: 153-191.

Maher, L.J., Heiri, O. and Lotter, A.F., 2012. Assessment of uncertainties associated with palaeolimnological laboratory methods and microfossil analysis. In *Tracking environmental change using lake sediments*. Springer, Dordrecht: 143-166.

Malhi, Y., Doughty, C.E., Galetti, M., Smith, F.A., Svenning, J-C. and Terborgh, J.W., 2016. Megafauna and ecosystem function from the Pleistocene to the Anthropocene, *Proceedings of the National Academy of Sciences*, 113(4): 838-846.

Marchant, R., Almeida, L., Behling, H., Berrio, J.C., Bush, M., Cleef, A., Duivenvoorden, J., Kappelle, M., De Oliveira, P., de Oliveira-Filho, A.T. and Lozano-Garćia, S., 2002. Distribution and ecology of parent taxa of pollen lodged within the Latin American Pollen database, *Review of Palaeobotany and Palynology*, 121(1): 1-75.

Marshall, L.G., Berta, A., Hoffstter, R., Pascual, R., Bombin, M. and Mones, A., 1984. Mammals and stratigraphy: geochronology of the continental mammal bearing Quaternary of South America. *Paleovertebrata, Mémoire Extraordinarie*. 1-76.

Martin, P.S and Klein, R.G., 1984. Prehistoric overkill: the global model. *Quaternary Extinctions: a prehistoric revolution*, Arizona, The University of Arizona Press: 354-403.

Martínez-Polanco, M. F., 2019. ‘Beyond White-tailed Deer Hunting in Aguazuque: Archaeofaunal Data from an Archaic Site at Sabana de Bogotá, Colombia’, *International Journal of Osteoarchaeology,* 29: 108–16.

MathWorks., 2019. *Matlab Software version R2019a* ed. MathsWorks, Natick, Massachusetts, USA.

Mergili, M., 2007. *Páramo El Ángel with frailejones*, The world in images, Piwigo, viewed 11 January 2022 <https://www.mergili.at/worldimages/picture.php?/8835>.

Mills, S. Soulé, M.E. and Doak, D.F., 1993. The Keystone-Species Concept in Ecology and Conservation, *BioScience*, 43(4): 219-224.

Munsell Colour Co., Inc., 1992, *Munsell soil colour charts* (revised ed.): Baltimore.

Neves, W.A. and Piló, L.B., 2003. Solving Lund's dilemma: new AMS dates confirm that humans and megafauna coexisted at Lagoa Santa. *Current Research in the Pleistocene*, 20:57-60.

Oksanen, J., 2009. Multivariate analysis of ecological communities in R: vegan tutorial. University of Oulu, Oulu.

Oksanen, J., Kindt, R., Legendre, P., O’Hara, B., Simpson, G.L., Solymos, P., Stevens, M.H.H., Wagner, H., 2007. *The vegan Package: Community Ecology Package*, R Foundation for Statistical Computing, Vienna.

Peres, C.A., Emilio, T., Schietti, J., Desmoulière, S.J. and Levi, T., 2016. Dispersal limitation induces long-term biomass collapse in overhunted Amazonian forests. *Proceedings of the National Academy of Sciences*, 113(4):892-897.

Perrotti, A.G. and van Asperen, E., 2019. Dung fungi as a proxy for megaherbivores: opportunities and limitations for archaeological applications, *Vegetation History and Archaeobotany,* 28: 93-104.

Perrotti, A.G., 2018. Pollen and *Sporormiella* evidence for terminal Pleistocene vegetation change and megafaunal extinction at Page-Ladson, Florida, *Quaternary International,* 466: 256-268.

Ponel, P., Court-Picon, M., Badura, M., Guiter, F., de Beaulieu, J.L., Andrieu-Ponel, V., Djamali, M., Leydet, M., Gandouin, E. and Buttler, A., 2011. Holocene history of Lac des Lauzons (2180 m asl), reconstructed from multiproxy analyses of Coleoptera, plant macroremains and pollen (Hautes-Alpes, France). *The Holocene*, 21(4): 565-582.

Poveda, G., Mesa, O.J., Salazar, L.F., Arias, P.A., Moreno, H.A., Vieira, S.C., Agudelo, P.A., Toro, V.G. and Alvarez, J.F., 2005. The diurnal cycle of precipitation in the tropical Andes of Colombia. *Monthly Weather Review*, 133(1): 228-240.

Poveda, G., Waylen, P.R. and Pulwarty, R.S., 2006. Annual and inter-annual variability of the present climate in northern South America and southern Mesoamerica. *Palaeogeography, Palaeoclimatology, Palaeoecology*, 234(1): 3-27.

Prado, J. L., Alberdi, M.T., Azanza, B., Sánchez, B. and Frassinetti, D., 2005. ‘The Pleistocene Gomphotheriidae (Proboscidea) from South America’. *Quaternary International*, 126-128: 21-30.

Prieto, A.R., 2000. Vegetational history of the Late glacial–Holocene transition in the grasslands of eastern Argentina. *Palaeogeography, Palaeoclimatology, Palaeoecology*, 157(3-4):167-188.

Pym, F.C., 2020. *The Timing and Ecosystem Consequences of Panama’s Late Pleistocene Functional Megafaunal Extinction*, University of Exeter, Exeter, unpublished.

Pym, F.C., Franco-Gaviria, F., Espinoza, I.G. and Urrego, D.H., 2022. The timing and ecological consequences of Pleistocene megafaunal collapse in the eastern Andes of Colombia, *Quaternary Research*, in review.

Raczka, M.F., Bush, M.B. and De Oliveira, P.D., 2018. The collapse of megafaunal populations in southeastern Brazil, *Quaternary Research*, 89: 103-118.

Raczka, M.F., Bush, M.B., Folcik, A.M. and McMichael, C.H., 2016. *Sporormiella* as a tool for detecting the presence of large herbivores in the Neotropics, *Biota Neotropica*, 16(1): 1-9.

Ramsey, C. B., 2009a. Bayesian analysis for radiocarbon dates, *Radiocarbon*, 51(1): 337-360.

Ramsey, C.B., 2009b. Dealing with outliers and offsets in radiocarbon dating, *Radiocarbon*, 51(3): 1023-1045.

Rangel-Ch, J.O., 2000. La Región Paramuna y franja Aledaña en Colombia, *Colombia biotic diversity III*. *La región de vida paramuna.* Bogotá, 1-23.

Raper, D. and Bush, M., 2009. A test of *Sporormiella* representation as a predictor of megaherbivore presence and abundance. *Quaternary Research*, 71(3): 490-496.

Reimer, P.J., Austin, W.E., Bard, E., Bayliss, A., Blackwell, P.G., Ramsey, C.B., Butzin, M., *et al.,* 2020. The IntCal20 Northern Hemisphere radiocarbon age calibration curve (0-55 cal kBP). *Radiocarbon,* 62: 725–757.

Revelles, J., Burjachs, F. and van Geel, B., 2016. 'Pollen and Non-Pollen Palynomorphs from the Early Neolithic Settlement of La Draga (Girona, Spain)'. *Review of Palaeobotany and Palynology* 225: 1-20.

Robinson, G.S. and Burney, D.A., 2008. The Hyde Park mastodon and palynological clues to megafaunal extinction. *Mastodon Paleobiology, Taphonomy, and Paleoenvironment in the Late Pleistocene of New York State: Studies on the Hyde Park, Chemung, and North Java Sites*, 61: 291-299.

Robinson, G.S., Burney, L.P and Burney, D.A., 2005. Landscape paleoecology and megafaunal extinction in southeastern New York State. *Ecological Monographs*, 75(3): 295-315.

Rodionov, S.N and Overland, J.E., 2005. Application of a sequential regime shift detection method to the Bering Seas ecosystem, *ICES Journal of Marine Science,* 62(3): 328-332.

Rodionov, S.N., 2004. A sequential algorithm for testing climate regime shifts, *Geophysical Research Letters,* 31(9). doi.org/10.1029/2004GL019448.

Rojas, E., Arce, B., Peña, A., Boshell, F. and Ayarza, M., 2010. Quantification and interpolation of local trends in temperature and precipitation in the high Andean areas of Cundinamarca and Boyacá (Colombia). *Revista Corpoica-Ciencia y Tecnologia Agropecuarias*, 11(2): 173-182.

Room, A., Franco-Gaviria, F. and Urrego, D.H., 2022. Package *rshift: paleoecology and regime shift analysis*. R package version 2.1.1. https://CRAN.Rproject.org/package=rshift [accessed 7 February 2022].

Rozas-Dávila, A., Valencia, B.G. and Bush, M., 2016. The functional extinction of Andean megafauna, *Ecology*, 97(10): 2533-2539.

RStudio Team., 2020. *RStudio: Integrated Development for R*, RStudio, PBC, Boston, Available at: <http://www.rstudio.com/>.

Rule, S., Brook, B.W., Haberle, S.G., Turnery, C.S.M., Kershaw, A.P. and Johnson, C.N., 2012. The Aftermath of Megafaunal Extinction: Ecosystem Transformation in Pleistocene Australia, *Science*, 335: 1483-1486.

Sánchez-Sánchez, H., Manjarrez, J., Domínguez-Tejada, C.A. and Morquecho-Contreras, A., 2015. Individual variance in the attributes of Clusia salvinii Donn.

Smith associated with the attraction of frugivores in the dispersal of fruits and seeds. *Revista Chapingo serieciencias forestales y del ambiente*, *21*(3): 307-316.

Sankaran, M., Hanan, N.P., Scholes, R.J., Ratnam, J., Augustine, D.J., Cade, B.S., Gignoux, J., Higgins, S.I., Le Roux, X., Ludwig, F. and Ardo, J., 2005. Determinants of woody cover in African savannas. *Nature*, 438(7069): 846-849.

Serrano, J., 2019. *A sacred lake, a swamp, and their forest*, accessed 19 January 2021, <http://sites.exeter.ac.uk/bioresilience/blog/2019/08/30/a-sacredlake aswamp-and-their-forest-2/#more-403>.

Service Layer Credits[a]: Source, Esri, Maxar, GeoEye, Earthstar Geographics, CNES/Airbus DS, USDA, USGS, AeroGRID, IGN, and the GIS User Community Esri, HERE, Garmin, (c) OpenStreetMap contributors, and the GIS user community.

Service Layer Credits[b]: Source: Esri, Maxar, GeoEye, Earthstar Geographics, CNES/Airbus DS, USDA, USGS, AeroGRID, IGN, and the GIS User Community.

Sharpj99., n.d. *Southern Bayberry (Morella cerifera L.)*, The Global Pollen Project, viewed 10 January 2022, <https://globalpollenproject.org/Taxon/Myricaceae/Morella/cerifera>.

Sylvester, S.P., Barrie, F.R. and Sylvester, M.D., 2018. Valeriana vilcabambensis (Valerianaceae), a New Species from Undisturbed Upper Montane Forest of the Southern Peruvian Andes. Novon: *A Journal for Botanical Nomenclature*, 26(1): 16-21.

Staver, A.C. and Bond, W.J., 2014. 'Is there a "Browse Trap"? Dynamics of herbivore impacts on trees and grasses in an African Savanna', *Journal of Ecology* 102(3): 595–602.

Steadman, D.W., Martin, P.S., MacPhee, R.D.E., Jull, A.J.T., McDonald, H.G., Woods, C.A., Iturralde-Vinent, M. and Hodgins, G.W.L., 2007. Early Holocene survival of megafauna in South America. *Journal of Biogeography*: 1642-1646.

Stockmarr, J.A., 1971. Tablets with spores used in absolute pollen analysis, *Pollen Spores*, 13: 615-621.

Stuart, A.J., 1999. Late Pleistocene megafaunal extinctions. *In Extinctions in near time*. Springer, Boston, MA.

The white deer., 2017. *A free downloadable white background picture of a deer*, HD wallpapers, viewed 04 January 2022, <https://www.allwhitebackground.com/?p=4845>.

Trachsel, M, and Telford, R.J., 2017. ‘All Age–Depth Models Are Wrong, but Are GettingBetter’. *The Holocene,* 27(6): 860–69.

Triana-Vega, A.V., Sedov, S., Salinas-Acero, J., Carvajal-Contreras, D., Moreano, C., Tovar–Reyes, M., Solleiro–Rebolledo, E. and Díaz-Ortega, J., 2019. Environmental reconstruction spanning the transition from hunter/gatherers to early farmers in Colombia: paleopedological and archaeological indicators from the pre-ceramic sites Tequendama and Aguazuque. *Quaternary international*, *516*: 175-189.

Ugueto, G.N., 2020. *Morning Warmup Sketch*, a concept sketch of the giant ground sloth *Eremotherium laurillardi,* Twitter for iPad, viewed 04 January 2022, <https://twitter.com/serpenillus/status/1297894174377877505>.

Urrego, D.H., Bush, M.B., Silman, M.R., Correa-Metrio, A.Y., Ledru, M.P., Mayle, F.E., Paduano, G. and Valencia, B.G., 2009. Millennial-scale ecological changes in tropical South America since the last glacial maximum. *In Past climate variability in South America and surrounding regions,* Springer, Dordrecht:283 300.

Urrego, D.H., Bush, M.B., Silman, M.R., Niccum, B.A., De La Rosa, P., McMichael, C.H., Hagen, S. and Palace, M., 2013. Holocene fires, forest stability and human occupation in south-western Amazonia. *Journal of biogeography*, 40(3): 521-533.

Urrego, D.H., Niccum, B.A., La Drew., C.F., Silman, M.R. and Bush. M.B., 2011a. ‘Fire and drought as drivers of Early Holocene tree line changes in the Peruvian Andes, *Journal of Quaternary Science*, 26(1): 28–36.

Urrego, D.H., Silman, M.R., Correa- Metrio, A. and Bush, M.B., 2011b. Pollen vegetation relationships along steep climatic gradients in western Amazonia. *Journal of Vegetation Science*, 22(5): 795-806.

van Asperen, E.N., Kirby, J.R. and Hunt, C.O., 2016. ‘The Effect of Preparation Methods on Dung Fungal Spores: Implications for Recognition of Megafaunal Populations’, *Review of Palaeobotany and Palynology* 229: 1-8.

van Asperen, E.N., Perrotti, A. and Baker, A., 2020. Coprophilous fungal spores: NPPs for the study of past megaherbivores, In *Applications of Non-Pollen Palynomorphs: from Palaeoenvironmental Reconstructions to Biostratigraphy*, Geological Society of London.

van der Hammen, T. and Correal-Urrego, G., 1978. Prehistoric man of the Sabana de Bogotá: Data for an ecological prehistory, *Palaeogeography, palaeoclimatology and palaeoecology*, 25: 179-190.

van der Hammen, T. and González, E., 1960. Upper Pleistocene and Holocene climate and vegetation of the “Sabana de Bogota” (Colombia, South America). *Leidse Geologische Mededelingen*, 25(1): 261-315.

van der Hammen, T. and González, E., 1960. Upper Pleistocene and Holocene climate and vegetation of the “Sabana de Bogotá” (Colombia, South America). *Leidse Geologische Mededelingen*, *25*(1): 261-315.

van der Hammen, T. and González, E., 1965. A late-glacial and holocene pollen diagram from Cienaga del Visitador (Dept. Boyaca, Colombia). *Leidse Geologische Mededelingen*, 32(1): 193-201.

van der Hammen, T., 1974. The Pleistocene Changes of Vegetation and Climate in Tropical South America, *Journal of Biogeography*, 1(1): 3-26.

van Geel, B., and van der Hammen, T., 1973. ‘Upper Quaternary Vegetational and Climatic Sequence of the Fuquene Area (Eastern Cordillera, Colombia)’, *Palaeogeography, Palaeoclimatology, Palaeoecology* 14(1): 9-92.

van Geel, B., Buurman, J., Brinkkemper, O., Schelvis, J., Aptroot, A., van Reenen, G. and Hakbijl, T., 2003. ‘Environmental Reconstruction of a Roman Period Settlement Site in Uitgeest (The Netherlands), with Special Reference to Coprophilous Fungi’. *Journal of Archaeological Science* 30(7): 873–83.

van Geel, B., Guthrie, R.D., Altmann, J.G., Broekens, P., Bull, I.D., Gill, F.L., Jansen, B., Nieman, A.M. and Gravendeel, B., 2011. Mycological evidence of coprophagy from the feces of an Alaskan Late Glacial mammoth. *Quaternary Science Reviews*, 30(17-18): 2289-2303.

van Geel, B., Zazula, G.D. and Schweger, C.E., 2007. Spores of coprophilous fungi from under the Dawson tephra (25,300 14C years BP), Yukon Territory, northwestern Canada, *Paleogeography, Palaeoclimatology, Palaeoecology*, 252: 481-485.

VancouverIslandGrows., 2018. *Cymes of Valierana Officinalis*, VancouverIslandGrows, viewed 12 January 2022, <https://vancouverislandgrows.wordpress.com/2018/01/23/valeriana officinalis/>.

Velásquez, C., Jojoa, L., Restrepo, A., Vergara. D., Samboni, V. and Castañeda, I., 2022. *Polynic catalogue of the Colombian Andes*, Colombia, unpublished.

Waldram, M.S., Bond, W.J. and Stock., W.D., 2008. ‘Ecological Engineering by a Mega Grazer: White Rhino Impacts on a South African Savanna’. *Ecosystems* 11(1): 101-112.

Waters, M.R., Forman, S.L., Jennings, T.A., Nordt, L.C., Driese, S.G., Feinberg, J.M., Keene, J.L., Halligan, J., Lindquist, A., Pierson, J. and Hallmark, C.T., 2011.

The Buttermilk Creek complex and the origins of Clovis at the Debra L. Friedkin site, Texas. *Science*, 331(6024): 1599-1603.

Whitlock, C. and Larsen, C., 2002. Charcoal as a Fire Proxy, in Tracking environmental change using lake sediments, Dordrecht, *Springer*: 75-97.

Wigley, B.J., Augustine, D.J., Coetsee, C., Ratnam, J. and Sankaran, M., 2020. Grasses continue to trump trees at soil carbon sequestration following herbivore exclusion in a semiarid African savanna. *Ecology*, 101(5).

Wood, J.R. and Wilmshurst, J.M., 2013. Accumulation rates or percentages? How to quantify *Sporormiella* and other coprophilous fungal spores to detect late Quaternary megafaunal extinction events. *Quaternary Science Reviews*, 77: 1-3.

Wroe, S., Field, J., Fullagar, R. and Jermin, L.S., 2004. Megafaunal extinction in the late Quaternary and the global overkill hypothesis, *Alcheringa*, 28(1): 291-331.

Zwerver, S-R., n.d. *Grote weegbree (Plantago) major ssp major 5*, Saxifraga – Free nature images, viewed 11 January 2022, <http://www.freenatureimages.eu/Plants/Flora%20OR/Plantago%20major%2C%20Greater%20Plantain/index.html>.